

A Student's Guide to and Review of Moment Tensors

M. L. Jost and R. B. Herrmann

*Department of Earth and Atmospheric Sciences
Saint Louis University
P. O. Box 8099
St. Louis, MO 63156*

ABSTRACT

A review of a moment tensor for describing a general seismic point source is presented to show a second order moment tensor can be related to simpler seismic source descriptions such as centers of expansion and double couples. A review of literature is followed by detailed algebraic expansions of the moment tensor into isotropic and deviatoric components. Specific numerical examples are provided in the appendices for use in testing algorithms for moment tensor decomposition.

INTRODUCTION

A major research interest in seismology is the description of the physics of seismic sources. A common approach is the approximation of seismic sources by a model of equivalent forces that correspond to the linear wave equations neglecting non-linear effects in the near source region (Geller, 1976; Aki and Richards, 1980; Kennett, 1983; Bullen and Bolt, 1985). Equivalent forces are defined as producing displacements at the earth's surface that are identical to those from the actual forces of the physical process at the source. The equivalent forces are determined from observed seismograms that contain information about the source and path and distortions due to the recording. Hence, the principle problem of source studies is the isolation of the source effect by correcting for instrument and path.

The classical method of describing seismic sources, having small dimensions compared to the wavelengths of interest (point source approximation) is by their strength (magnitudes, seismic moment) and their fault plane solution (Honda, 1962; Hirasawa and Stauder, 1965; Herrmann, 1975). Recently, seismic moment tensors have been used routinely for describing seismic point sources (e.g. Kanamori and Given, 1982; Dziewonski and Woodhouse, 1983b; Dziewonski *et al.*, 1983a-c, 1984a-c; Giardini, 1984; Ekström and Dziewonski, 1985; Dziewonski *et al.*, 1985a-d, 1986a-c, 1987a-f; Ekström *et al.*, 1987; Sipkin, 1987; PDE monthly listings published by NEIS). Gilbert (1970) introduced moment tensors for calculating the displacement at the free surface which can be expressed as a sum of moment tensor elements times the corresponding Green's function. An elastodynamic Green's function is a displacement field due to an unidirectional unit impulse, i.e. the Green's function is the impulse response of the medium between source and receiver. The response of the medium to any other time function is the convolution (Arfken, 1985) of that time function with the impulse response. The Green's function depends on source and receiver coordinates, the earth model, and is a tensor (Aki and Richards, 1980). The linearity between the moment tensor and Green's function elements was first used by Gilbert (1973) for calculating moment tensor elements from observations (moment tensor inversion). The concept of seismic moment tensors

was further extended by Backus and Mulcahy (1976), and Backus (1977a, b). Moment tensors can be determined from free oscillations of the earth (e.g. Gilbert and Dziewonski, 1975), long-period surface waves (e.g. McCowan, 1976; Mendiguren, 1977; Patton and Aki, 1979; Patton, 1980; Kanamori and Given, 1981, 1982; Romanowicz, 1981; Lay *et al.*, 1982; Nakanishi and Kanamori, 1982, 1984) or long-period body waves (e.g. Stump and Johnson, 1977; Strelitz, 1978, 1980; Ward, 1980a, b; Fitch *et al.*, 1980; Fitch, 1981; Langston, 1981; Dziewonski *et al.*, 1981; Dziewonski and Woodhouse, 1983a, b). Throughout this Student's Guide, we will focus on second-rank, time independent moment tensors (Appendix I). We refer to Dziewonski and Gilbert (1974), Gilbert and Dziewonski (1975), Backus and Mulcahy (1976), Backus (1977a), Stump and Johnson (1977), Strelitz (1980), Sipkin (1982), and Vasco and Johnson (1988) for a description of time dependent moment tensors. Higher order moment tensors are discussed by Backus and Mulcahy (1976), Backus (1977a, b), and Dziewonski and Woodhouse (1983a).

The reason that moment tensors are important is that they completely describe in a first order approximation the equivalent forces of general seismic point sources. The equivalent forces can be correlated to physical source models such as sudden relative displacement at a fault surface (elastic rebound model by H. F. Reid, 1910), rapidly propagating metastable phase transitions (Evison, 1963), sudden volume collapse due to phase transitions, or sudden volume increase due to explosions (Kennett, 1983; Vasco and Johnson, 1988). The equivalent forces representing a sudden displacement on a fault plane form the familiar double couple. The equivalent forces of a sudden change in shear modulus in presence of axial strain are represented by a linear vector dipole (Knopoff and Randall, 1970). In conclusion, a seismic moment tensor is a general concept, describing a variety of seismic source models, the shear dislocation (double couple source) being just one of them.

The equivalent forces can be determined from an analysis of the eigenvalues and eigenvectors of the moment tensor (Appendix I). The sum of the eigenvalues of the moment tensor describes the volume change in the source (isotropic component of the moment tensor). If the

sum is positive, the isotropic component is due to an explosion. The source has an implosive component if the sum is negative. If the sum of the eigenvalues vanishes, then the moment tensor has only deviatoric components. The deviatoric moment tensor represents a pure double couple source if one eigenvalue equals zero. If none of the eigenvalues vanishes and their sum still equals zero, the moment tensor can be decomposed into a major and minor double couple (Kanamori and Given, 1981), or a double couple and a compensated linear vector dipole (CLVD) (Knopoff and Randall, 1970). A CLVD is a dipole that is corrected for the effect of volume change, describing seismic sources which have no volume change, net force, or net moment. In general, a complete moment tensor can be the superposition of an isotropic component and three vector dipoles (or three CLVD's, or three double couples, Ben-Menahem and Singh, 1981).

This Student's Guide is an extension of "A student's guide to the use of P- and S- wave data for focal mechanism determination" (Herrmann, 1975). Hence, emphasis is given illustrating the relations between classical fault plane solutions and seismic moment tensors. Addressing general seismic point sources, we provide examples of moment tensor decompositions into basic equivalent source representations, as contributions of dipoles or double couple sources. Clarification of terms such as major and minor double couple or compensated linear vector dipole is provided. Moment tensor inversion schemes are briefly summarized. In the appendices, examples of the use of notation by different authors are given along with some numerical results which are useful for testing computer programs. Furthermore, the formulation of the basic Green's functions by Herrmann and Wang (1985) is connected to a simple moment tensor inversion scheme.

GENERAL ELASTODYNAMIC SOURCE

By using the representation theorem for seismic sources (Aki and Richards, 1980), the observed displacement d_n at an arbitrary position \mathbf{x} at the time t due to a distribution of equivalent body force densities, f_k , in a source region is

$$d_n(\mathbf{x}, t) = \int_{-\infty}^{\infty} \int_V G_{nk}(\mathbf{x}, t; \mathbf{r}, \bar{t}) f_k(\mathbf{r}, \bar{t}) dV(\mathbf{r}) d\bar{t}, \quad (1)$$

where G_{nk} are the components of the Green's function containing the propagation effects, and V is the source volume where f_k are non-zero. We assume the summation convention for repeated indices (Arfken, 1985). The subscript n indicates the component of the displacement. Throughout, we will use the following coordinate system (Figure 1): The x-axis points towards north, the y-axis towards east, and the z-axis down (this system is right handed). Then, \mathbf{e}_x , \mathbf{e}_y , and \mathbf{e}_z are the unit vectors towards north, east, and vertically down, respectively.

By assuming that the Green's functions vary smoothly within the source volume in the range of moderate frequencies, the Green's functions can be expanded into a Taylor series around a reference point to facilitate the spatial integration in (1) (Kennett, 1983; Arfken, 1985). The expansion is usually done around the centroid $\mathbf{r} = \xi$. The physical source region is characterized by the existence of the equivalent forces. These forces

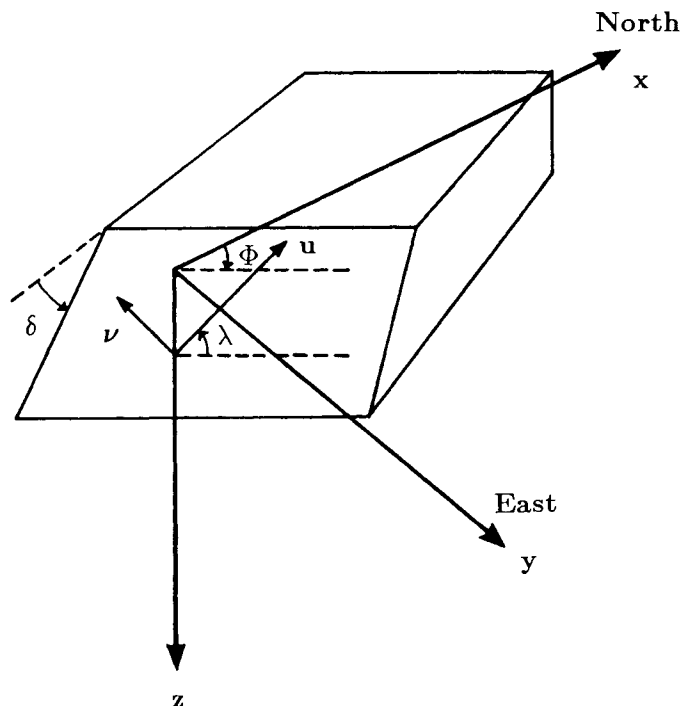


Fig. 1. Definition of the Cartesian coordinates (x, y, z) . The origin is at the epicenter. Strike is measured clockwise from north, dip from horizontal down, and slip counterclockwise from horizontal. \mathbf{u} and \mathbf{v} are the slip vector and fault normal, respectively (modified after Aki and Richards, 1980).

arise due to differences between the model stress and the actual physical stress (stress glut, Backus and Mulcahy, 1976). Outside the source region, the stress glut vanishes as do the equivalent forces. The centroid of the stress glut is then a weighted mean position of the physical source region (Backus, 1977a; Aki and Richards, 1980; Dziewonski and Woodhouse, 1983a). It seems that the centroid of the stress glut gives a better position for the equivalent point source of an earthquake than the hypocenter which describes just the position of rupture initialization. The Taylor series expansion of the components of the Green's function around this new reference point is

$$G_{nk}(\mathbf{x}, t; \mathbf{r}, \bar{t}) = \sum_{m=0}^{\infty} \frac{1}{m!} (r_{j_1} - \xi_{j_1}) \cdots (r_{j_m} - \xi_{j_m}) G_{nk, j_1 \dots j_m}(\mathbf{x}, t; \xi, \bar{t}). \quad (2)$$

The comma between indices in (2) describes partial derivatives with respect to the coordinates after the comma. We define the components of the time dependent force moment tensor as :

$$M_{kj_1 \dots j_m}(\xi, \bar{t}) = \int_V (r_{j_1} - \xi_{j_1}) \cdots (r_{j_m} - \xi_{j_m}) f_k(\mathbf{r}, \bar{t}) dV. \quad (3)$$

If conservation of linear momentum applies, such as for a source in the interior of a body, then a term in M_k does not exist in (3). With the Taylor expansion (2) and the definition of the time dependent moment tensor (3), the displacement (1) can be written as a sum of terms which resolve additional details of the source (multipole expansion).

sion, Backus and Mulcahy, 1976; Stump and Johnson, 1977; Aki and Richards, 1980; Kennett, 1983; Dziewonski and Woodhouse, 1983a; Vasco and Johnson, 1988):

$$d_n(\mathbf{x}, t) = \sum_{m=1}^{\infty} \frac{1}{m!} G_{nk, j_1 \dots j_m}(\mathbf{x}, t, \xi, \bar{t}) * M_{kj_1 \dots j_m}(\xi, \bar{t}), \quad (4)$$

where $*$ denotes the temporal convolution. By using a seismic signal that has much longer wavelengths than the dimensions of the source (point source approximation), we need to consider only the first term in (4) (Backus and Mulcahy, 1976; Stump and Johnson, 1977). Note, that single forces will not be present in (4) if there are no externally applied forces (indigenous source). The total force, linear and angular momentum must vanish for the equivalent forces of an indigenous source (Backus and Mulcahy, 1976). The conservation of angular momentum for the equivalent forces leads to the symmetry of the seismic moment tensor (Gilbert, 1970).

We assume that all components of the time dependent seismic moment tensor in (4) have the same time dependence $s(\bar{t})$ (synchronous source, Silver and Jordan,

1982). Neglecting higher order terms, we get (Stump and Johnson, 1977)

$$d_n(\mathbf{x}, t) = M_{kj} [G_{nk, j} * s(\bar{t})] \quad (5)$$

M_{kj} are constants representing the components of the second order seismic moment tensor \mathbf{M} , usually termed *the* moment tensor. Note that the displacement d_n is a linear function of the moment tensor elements and the terms in the square brackets. If the source time function $s(t)$ is a delta function, the only term left in the square brackets is $G_{nk, j}$ describing nine generalized couples. The derivative of a Green's function component with respect to the source coordinate ξ_j is equivalent to a single couple with arm in the ξ_j direction. For $k = j$, i.e. force in the same direction as the arm, the generalized couples are vector dipoles (Figure 2; Maruyama, 1964). Thus, the moment tensor component M_{kj} gives the excitation of the generalized (k,j) couple.

DOUBLE COUPLE SOURCES

The moment tensor components in (5) in an isotropic medium for a double couple of equivalent forces are given by

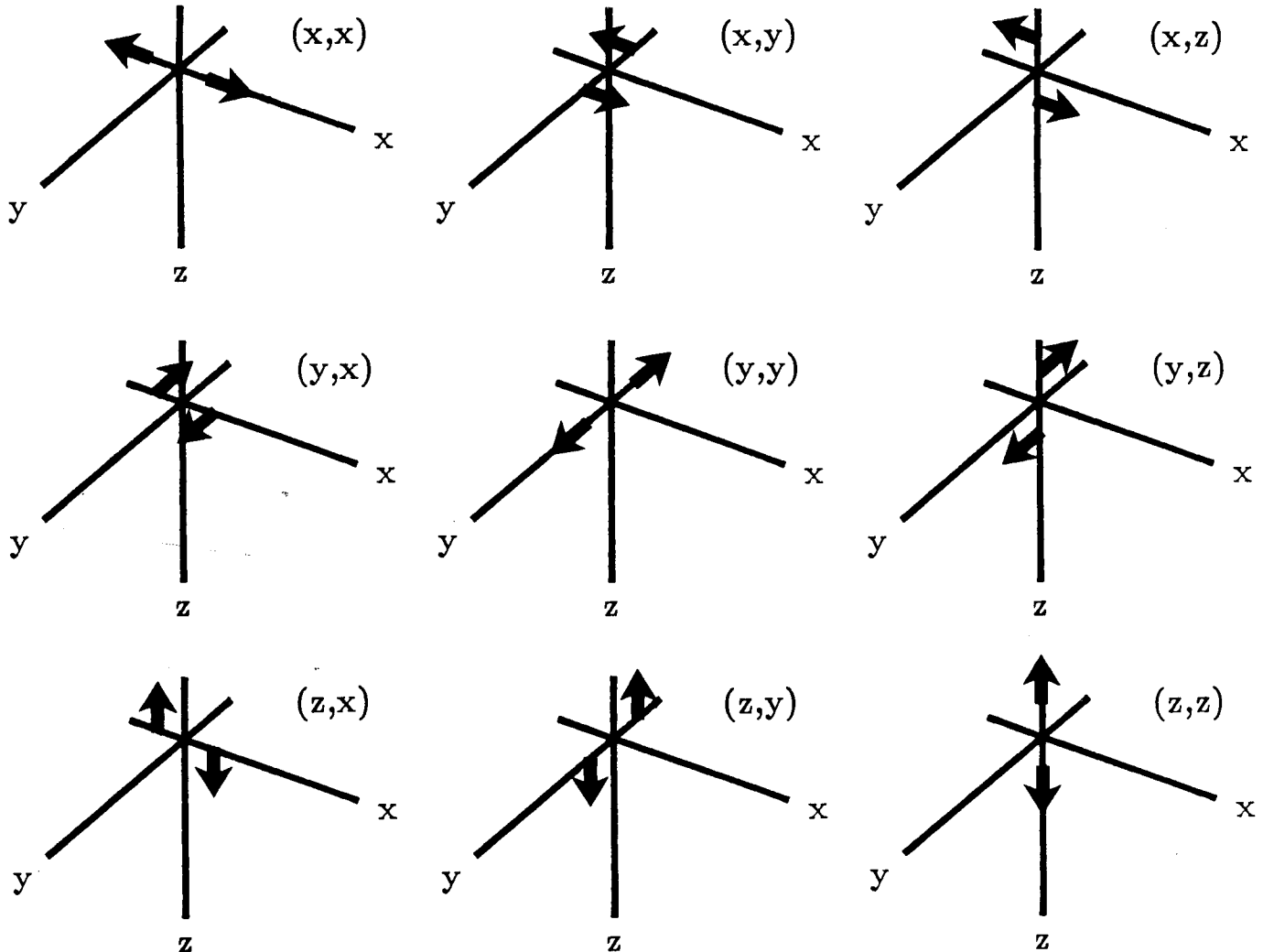


Fig. 2. The nine generalized couples representing $G_{nk, j}$ in (5) (modified after Aki and Richards, 1980).

$$M_{kj} = \mu A (u_k \nu_j + u_j \nu_k) , \quad (6)$$

where μ is the shear modulus, A is the area of the fault plane, \mathbf{u} denotes the slip vector on the fault surface, and $\boldsymbol{\nu}$ is the vector normal to the fault plane (Aki and Richards, 1980; Ben-Menahem and Singh, 1981). Note that the contributions of the vector of the fault normal $\boldsymbol{\nu}$ and the slip vector \mathbf{u} are symmetric in (6). From the symmetry of \mathbf{M} , we note that the roles of the vectors \mathbf{u} and $\boldsymbol{\nu}$ could be interchanged without affecting the displacement field; i.e. the fault normal could equivalently be the slip vector and vice versa. This well known fault plane - auxiliary plane ambiguity cannot be resolved from the seismic radiation of a point source. Hence studies of locations of aftershocks, surface faulting, rupture directivity, or static final displacements (Backus, 1977a) need to be done in order to resolve this ambiguity.

The term $u_k \nu_j + u_j \nu_k$ in (6) forms a tensor, \mathbf{D} , describing a double couple. This tensor is real and symmetric, giving real eigenvalues and orthogonal eigenvectors (Appendix I). The eigenvalues are proportional to (1, 0, -1). Hence, the characteristic properties of a moment tensor representing a double couple are i) one eigenvalue of the moment tensor vanishes, and ii) the sum of the eigenvalues vanishes, i.e. the trace of the moment tensor is zero (the other two eigenvalues are constrained to equal magnitude but opposite sign).

Let \mathbf{t} , \mathbf{b} , and \mathbf{p} designate the orthogonal eigenvectors to the above eigenvalues (Herrmann, 1975; Backus, 1977a; Dziewonski and Woodhouse, 1983a).

$$\mathbf{t} = \frac{1}{\sqrt{2}} (\boldsymbol{\nu} + \mathbf{u}) \quad (7)$$

$$\mathbf{b} = \boldsymbol{\nu} \times \mathbf{u} \quad (8)$$

$$\mathbf{p} = \frac{1}{\sqrt{2}} (\boldsymbol{\nu} - \mathbf{u}) . \quad (9)$$

The tensor \mathbf{D} corresponding to the terms in the brackets in (6) can be diagonalized (principal axis transformation, see Appendix I), where the eigenvectors give the directions of the principal axes. The eigenvector \mathbf{b} corresponding to the eigenvalue zero gives the null-axis, the eigenvector \mathbf{t} corresponding to the positive eigenvalue gives the tension axis, T, and the eigenvector \mathbf{p} corresponding to the negative eigenvalue gives the pressure axis, P, of the tensor. These axes can be related to the corresponding axes of the fault plane solution, since we are focusing on pure double couple sources. The P-axis is in the direction of maximum compressive motion on the fault surface; the T-axis is the direction of maximum tensional motion. Note that the P- and T-axes inferred from the motion on the fault surface are not necessarily identical to the axes of maximum tectonic stress, since the motion can be on a preexisting plane of weakness rather than on a newly formed fault plane that would correspond to the maximum tectonic stress (McKenzie, 1969). However, this ambiguity cannot be resolved from the seismic radiation. In order to determine the direction of maximum tectonic stress, additional geological data such as *in situ* stress measurements and frictional forces is necessary. Lacking this kind of information, it is generally assumed that the P- and T- axes found from the seismic wave radiation are somewhat indicative of the direction of tectonic stress.

The double couple $u_k \nu_j + u_j \nu_k$ can equivalently be described by its eigenvectors (Gilbert, 1973).

$$u_k \nu_j + u_j \nu_k = t_k t_j - p_j p_k \quad (10)$$

$$= 0.5 [(t_k + p_k)(t_j - p_j) + (t_k - p_k)(t_j + p_j)] .$$

Comparing the terms in (10), we find the relation between tension and pressure axes and slip vector and fault normal (Appendix I):

$$\mathbf{u} = \frac{1}{\sqrt{2}} (\mathbf{t} + \mathbf{p}) \quad (11)$$

$$\boldsymbol{\nu} = \frac{1}{\sqrt{2}} (\mathbf{t} - \mathbf{p}) . \quad (12)$$

The other nodal plane is defined by

$$\mathbf{u} = \frac{1}{\sqrt{2}} (\mathbf{t} - \mathbf{p}) \quad (13)$$

$$\boldsymbol{\nu} = \frac{1}{\sqrt{2}} (\mathbf{t} + \mathbf{p}) . \quad (14)$$

If strike, Φ , dip, δ , and slip, λ , of the faulting are known, the slip vector \mathbf{u} and the fault normal $\boldsymbol{\nu}$ are given by (Aki and Richards, 1980)

$$\mathbf{u} = \bar{u} (\cos \lambda \cos \Phi + \cos \delta \sin \lambda \sin \Phi) \mathbf{e}_x$$

$$+ \bar{u} (\cos \lambda \sin \Phi - \cos \delta \sin \lambda \cos \Phi) \mathbf{e}_y \quad (15)$$

$$- \bar{u} \sin \delta \sin \lambda \mathbf{e}_z ,$$

where \bar{u} is the mean displacement on the fault plane. The fault normal $\boldsymbol{\nu}$ is

$$\boldsymbol{\nu} = -\sin \delta \sin \Phi \mathbf{e}_x + \sin \delta \cos \Phi \mathbf{e}_y - \cos \delta \mathbf{e}_z . \quad (16)$$

The scalar product of \mathbf{u} and $\boldsymbol{\nu}$ is zero. The strike of the fault plane, Φ , is measured clockwise from north, with the fault plane dipping to the right when looking along the strike direction. Equivalently, the hanging wall is then to the right (Figure 1). The dip, δ , is measured down from the horizontal. The slip, λ , is the angle between the strike direction and the direction the hanging wall moved relative to the foot wall (the slip is positive when measured counterclockwise as viewed from the hanging wall side). The range of the fault orientation parameters are $0 \leq \Phi \leq 2\pi$, $0 \leq \delta \leq \frac{\pi}{2}$, and $-\pi \leq \lambda \leq \pi$ (Herrmann, 1975; Aki and Richards, 1980). The scalar seismic moment is

$$M_o = \mu A \bar{u} . \quad (17)$$

Equation (6) together with (15), (16), and (17) lead to the Cartesian components of the symmetric moment tensor in terms of strike, dip, and slip angles.

$$M_{xx} = -M_o (\sin \delta \cos \lambda \sin 2\Phi + \sin 2\delta \sin \lambda \sin^2 \Phi)$$

$$M_{yy} = M_o (\sin \delta \cos \lambda \sin 2\Phi - \sin 2\delta \sin \lambda \cos^2 \Phi)$$

$$M_{zz} = M_o (\sin 2\delta \sin \lambda) \quad (18)$$

$$M_{xy} = M_o (\sin \delta \cos \lambda \cos 2\Phi + 0.5 \sin 2\delta \sin \lambda \sin 2\Phi)$$

$$M_{xz} = -M_o (\cos \delta \cos \lambda \cos \Phi + \cos 2\delta \sin \lambda \sin \Phi)$$

$$M_{yz} = -M_o (\cos \delta \cos \lambda \sin \Phi - \cos 2\delta \sin \lambda \cos \Phi)$$

Different notation of the moment tensor elements are discussed in Appendix II. In Appendix III, several simple

A Student's Guide to and Review of Moment Tensors

moment tensors are related to fault plane solutions. Body-wave and surface wave radiation patterns from a source represented by a moment tensor are discussed by Kennett (1988).

Since the seismic moment tensor is real and symmetric, a principal axis transformation can be found, diagonalizing \mathbf{M} (Appendix I). The diagonal elements are the eigenvalues m_i of \mathbf{M} . Then, the scalar seismic moment can be determined from a given moment tensor by

$$M_0 = \frac{1}{2} (|m_1| + |m_2|) , \quad (19)$$

where m_1 and m_2 are the largest eigenvalues (in the absolute sense). The seismic moment can equivalently be estimated by the relations (Silver and Jordan, 1982):

$$M_0 = \left(\frac{\sum M_{kj}^2}{2} \right)^{\frac{1}{2}} = \left(\frac{\sum m_i^2}{2} \right)^{\frac{1}{2}} . \quad (20)$$

GENERAL SEISMIC POINT SOURCES

In this section, it is assumed that the seismic source *cannot* be described by a pure double couple mechanism. The moment tensor is represented as sum of an isotropic part, which is a scalar times the identity matrix, and a deviatoric part.

In order to derive a general formulation of the moment tensor decomposition, let's consider the eigenvalues and orthonormal eigenvectors of the moment tensor. Let m_i be the eigenvalue corresponding to the orthonormal eigenvector $\mathbf{a}_i = (a_{ix}, a_{iy}, a_{iz})^T$. Using the orthonormality of the eigenvectors (Appendix I, (A1.5)), we can write the principal axis transformation of \mathbf{M} in reverse order as:

$$\mathbf{M} = \begin{bmatrix} \mathbf{a}_1 & \mathbf{a}_2 & \mathbf{a}_3 \end{bmatrix} \mathbf{m} \begin{bmatrix} \mathbf{a}_1^T \\ \mathbf{a}_2^T \\ \mathbf{a}_3^T \end{bmatrix} \quad (21)$$

$$= \begin{bmatrix} a_{1x} & a_{2x} & a_{3x} \\ a_{1y} & a_{2y} & a_{3y} \\ a_{1z} & a_{2z} & a_{3z} \end{bmatrix} \begin{bmatrix} m_1 & 0 & 0 \\ 0 & m_2 & 0 \\ 0 & 0 & m_3 \end{bmatrix} \begin{bmatrix} a_{1x} & a_{1y} & a_{1z} \\ a_{2x} & a_{2y} & a_{2z} \\ a_{3x} & a_{3y} & a_{3z} \end{bmatrix} .$$

From (21), we find relations between components of the eigenvectors and moment tensor elements:

$$\begin{aligned} M_{xx} &= m_1 a_{1x}^2 + m_2 a_{2x}^2 + m_3 a_{3x}^2 \\ M_{yy} &= m_1 a_{1y}^2 + m_2 a_{2y}^2 + m_3 a_{3y}^2 \\ M_{zz} &= m_1 a_{1z}^2 + m_2 a_{2z}^2 + m_3 a_{3z}^2 \\ M_{xy} &= m_1 a_{1x} a_{1y} + m_2 a_{2x} a_{2y} + m_3 a_{3x} a_{3y} \\ M_{xz} &= m_1 a_{1x} a_{1z} + m_2 a_{2x} a_{2z} + m_3 a_{3x} a_{3z} \\ M_{yz} &= m_1 a_{1y} a_{1z} + m_2 a_{2y} a_{2z} + m_3 a_{3y} a_{3z} . \end{aligned} \quad (22)$$

The effect of the eigenvalue decomposition (21) is that a new orthogonal coordinate system, given by the eigenvectors, has been defined. In this new coordinate system, the source excitation is completely described by a linear combination of these orthogonal dipole sources.

\mathbf{m} in (21) is the diagonalized moment tensor. The elements of \mathbf{m} are the eigenvalues of \mathbf{M} . We now define the

general moment tensor decomposition by rewriting \mathbf{m} as

$$\begin{aligned} \mathbf{m} &= \frac{1}{3} \begin{bmatrix} \text{tr}(\mathbf{M}) & 0 & 0 \\ 0 & \text{tr}(\mathbf{M}) & 0 \\ 0 & 0 & \text{tr}(\mathbf{M}) \end{bmatrix} \\ &+ \begin{bmatrix} m_1^* & 0 & 0 \\ 0 & m_2^* & 0 \\ 0 & 0 & m_3^* \end{bmatrix} \\ &= \frac{1}{3} \begin{bmatrix} \text{tr}(\mathbf{M}) & 0 & 0 \\ 0 & \text{tr}(\mathbf{M}) & 0 \\ 0 & 0 & \text{tr}(\mathbf{M}) \end{bmatrix} + \sum_{i=1}^N \overline{\mathbf{m}}_i , \end{aligned} \quad (23)$$

where $\text{tr}(\mathbf{M}) = m_1 + m_2 + m_3$ is the trace of the moment tensor and $\overline{\mathbf{m}}_i$ is a set of diagonal matrices whose sum yields the second term in (23). The purely deviatoric eigenvalues m_i^* of the moment tensor are

$$m_i^* = m_i - \frac{m_1 + m_2 + m_3}{3} = m_i - \frac{1}{3} \text{tr}(\mathbf{M}) . \quad (24)$$

The first term on the right hand side (RHS) of (23) describes the isotropic part of the moment tensor. The eigenvalues of the isotropic part of the moment tensor are important for quantifying a volume change in the source. The second term describes the deviatoric part of the moment tensor consisting of purely deviatoric eigenvalues, which are calculated by subtracting $1/3 \text{tr}(\mathbf{M})$ from each eigenvalue of \mathbf{M} . This deviatoric part of the moment tensor can be further decomposed, where the number of terms or the specific form of the decomposition will be discussed in the next sections. Obviously, a multitude of different decompositions are possible. In Appendix IV, we give some numerical examples illustrating several methods of moment tensor decomposition.

Vector Dipoles

A moment tensor can be decomposed into an isotropic part and three vector dipoles. In equation (23) let $N = 3$ and

$$\overline{\mathbf{m}}_1 = \begin{bmatrix} m_1^* & 0 & 0 \\ 0 & 0 & 0 \\ 0 & 0 & 0 \end{bmatrix}, \quad \overline{\mathbf{m}}_2 = \begin{bmatrix} 0 & 0 & 0 \\ 0 & m_2^* & 0 \\ 0 & 0 & 0 \end{bmatrix}, \quad \overline{\mathbf{m}}_3 = \begin{bmatrix} 0 & 0 & 0 \\ 0 & 0 & 0 \\ 0 & 0 & m_3^* \end{bmatrix} . \quad (25)$$

Applying (21) to $\overline{\mathbf{m}}_1$, we get for the first deviatoric term ($i=1$) in the decomposition

$$m_1^* \begin{bmatrix} a_{1x}^2 & a_{1x} a_{1y} & a_{1x} a_{1z} \\ a_{1x} a_{1y} & a_{1y}^2 & a_{1y} a_{1z} \\ a_{1x} a_{1z} & a_{1y} a_{1z} & a_{1z}^2 \end{bmatrix} = m_1^* \mathbf{a}_1 \mathbf{a}_1 , \quad (26)$$

where we identified the matrix as the dyadic $\mathbf{a}_1 \mathbf{a}_1$ (Appendix I). The dyadic $\mathbf{a}_1 \mathbf{a}_1$ describes a dipole in the direction of the eigenvector \mathbf{a}_1 . By applying (21) to $\overline{\mathbf{m}}_2$ and $\overline{\mathbf{m}}_3$ in (25), we get similar expressions involving $\mathbf{a}_2 \mathbf{a}_2$ and $\mathbf{a}_3 \mathbf{a}_3$, describing the second and third deviatoric terms in the decomposition. Finally, equation (21) can be written for the decomposition into three linear vector dipoles along the directions of the eigenvectors of \mathbf{M} as

$$\mathbf{M} = \frac{1}{3}(m_1+m_2+m_3)\mathbf{I} + m_1^* \mathbf{a}_1\mathbf{a}_1 + m_2^* \mathbf{a}_2\mathbf{a}_2 + m_3^* \mathbf{a}_3\mathbf{a}_3, \quad (27)$$

which is identical to (22) and equation (4.55) in Ben-Menahem and Singh (1981).

Double Couples

Next, we decompose a moment tensor into an isotropic part and three double couples. For the deviatoric part in (23) let $N = 6$ and

$$\begin{aligned} \bar{\mathbf{m}}_1 &= \frac{1}{3} \begin{bmatrix} m_1^* & 0 & 0 \\ 0 & -m_1^* & 0 \\ 0 & 0 & 0 \end{bmatrix}, & \bar{\mathbf{m}}_2 &= \frac{1}{3} \begin{bmatrix} m_1^* & 0 & 0 \\ 0 & 0 & 0 \\ 0 & 0 & -m_1^* \end{bmatrix} \\ \bar{\mathbf{m}}_3 &= \frac{1}{3} \begin{bmatrix} 0 & 0 & 0 \\ 0 & m_2^* & 0 \\ 0 & 0 & -m_2^* \end{bmatrix}, & \bar{\mathbf{m}}_4 &= \frac{1}{3} \begin{bmatrix} -m_2^* & 0 & 0 \\ 0 & m_2^* & 0 \\ 0 & 0 & 0 \end{bmatrix} \\ \bar{\mathbf{m}}_5 &= \frac{1}{3} \begin{bmatrix} 0 & 0 & 0 \\ 0 & -m_3^* & 0 \\ 0 & 0 & m_3^* \end{bmatrix}, & \bar{\mathbf{m}}_6 &= \frac{1}{3} \begin{bmatrix} -m_3^* & 0 & 0 \\ 0 & 0 & 0 \\ 0 & 0 & m_3^* \end{bmatrix}, \end{aligned} \quad (28)$$

where each $\bar{\mathbf{m}}_i$ is equivalent to a pure double couple source (Appendix III). Notice that each double couple consists of two linear vector dipoles (c.f. (25), (26) and (28)), e.g. $(m_1^*/3)(\mathbf{a}_1\mathbf{a}_1 - \mathbf{a}_2\mathbf{a}_2)$ for $\bar{\mathbf{m}}_1$. Each dipole consists of two forces of equal strength but opposite direction (c.f. Figure 2). Then, the double couple can be seen this way: The first couple is formed by one force of each dipole, one force pointing in the positive \mathbf{a}_1 , the other in the negative \mathbf{a}_2 direction. The corresponding other couple is constructed by the complementary force of each dipole, pointing toward the negative \mathbf{a}_1 and positive \mathbf{a}_2 direction.

Using (21) with (23) and (28), we get the result that a moment tensor can be decomposed into an isotropic part and three double couples.

$$\begin{aligned} \mathbf{M} &= \frac{1}{3}(m_1+m_2+m_3)\mathbf{I} + \frac{1}{3}(m_1-m_2)(\mathbf{a}_1\mathbf{a}_1 - \mathbf{a}_2\mathbf{a}_2) \\ &+ \frac{1}{3}(m_2-m_3)(\mathbf{a}_2\mathbf{a}_2 - \mathbf{a}_3\mathbf{a}_3) + \frac{1}{3}(m_3-m_1)(\mathbf{a}_3\mathbf{a}_3 - \mathbf{a}_1\mathbf{a}_1), \end{aligned} \quad (29)$$

which is identical to equation (4.57) in Ben-Menahem and Singh (1981).

CLVD

Alternatively, a moment tensor can be decomposed into an isotropic part and three compensated linear vector dipoles. Adding terms like $\bar{\mathbf{m}}_1$ and $\bar{\mathbf{m}}_2$ in (28) gives a CLVD, $2\mathbf{a}_1\mathbf{a}_1 - \mathbf{a}_2\mathbf{a}_2 - \mathbf{a}_3\mathbf{a}_3$. This CLVD represents a dipole of strength 2 in the direction of the eigenvector \mathbf{a}_1 , and two dipoles of unit strength in the directions of the eigenvectors \mathbf{a}_2 and \mathbf{a}_3 , respectively. The decomposition can then be expressed as:

$$\begin{aligned} \mathbf{M} &= \frac{1}{3}(m_1+m_2+m_3)\mathbf{I} + \frac{1}{3}m_1(2\mathbf{a}_1\mathbf{a}_1 - \mathbf{a}_2\mathbf{a}_2 - \mathbf{a}_3\mathbf{a}_3) \\ &+ \frac{1}{3}m_2(2\mathbf{a}_2\mathbf{a}_2 - \mathbf{a}_1\mathbf{a}_1 - \mathbf{a}_3\mathbf{a}_3) + \frac{1}{3}m_3(2\mathbf{a}_3\mathbf{a}_3 - \mathbf{a}_1\mathbf{a}_1 - \mathbf{a}_2\mathbf{a}_2), \end{aligned} \quad (30)$$

which is identical to equation (4.56) in Ben-Menahem and Singh (1981).

Major and Minor Couple

Next, we will decompose a moment tensor into an isotropic component, a major and minor double couple. The major couple seems to be the best approximation of a general seismic source by a double couple (Appendix IV), since the directions of the principal axes of the moment tensor remain unchanged. The major double couple is constructed in the following way (Kanamori and Given, 1981; Wallace, 1985): The eigenvector of the smallest eigenvalue (in the absolute sense) is taken as the null-axis. Let's assume that $|m_3^*| \geq |m_2^*| \geq |m_1^*|$ in (23). In (23), let $N=2$ and use the deviatoric condition $m_1^* + m_2^* + m_3^* = 0$ to obtain

$$\bar{\mathbf{m}}_1 = \begin{bmatrix} 0 & 0 & 0 \\ 0 & -m_3^* & 0 \\ 0 & 0 & m_3^* \end{bmatrix}, \quad \bar{\mathbf{m}}_2 = \begin{bmatrix} m_1^* & 0 & 0 \\ 0 & -m_1^* & 0 \\ 0 & 0 & 0 \end{bmatrix}. \quad (31)$$

Applying (21) to $\bar{\mathbf{m}}_1$, we get the first deviatoric term in the decomposition which corresponds to a pure double couple termed *major couple*.

$$\mathbf{M}^{MAJ} = \begin{bmatrix} \mathbf{a}_1 & \mathbf{a}_2 & \mathbf{a}_3 \end{bmatrix} \begin{bmatrix} 0 & 0 & 0 \\ 0 & -m_3^* & 0 \\ 0 & 0 & m_3^* \end{bmatrix} \begin{bmatrix} \mathbf{a}_1^T \\ \mathbf{a}_2^T \\ \mathbf{a}_3^T \end{bmatrix}. \quad (32)$$

Instead of the *major* double couple, a *best* double couple can be constructed similarly by replacing m_3^* in (32) by the average of the largest two eigenvalues (in the absolute sense, Giardini, 1984). Applying (21) to $\bar{\mathbf{m}}_2$ gives the second deviatoric term in the decomposition which also corresponds to a pure double couple termed *minor couple*.

$$\mathbf{M}^{MIN} = \begin{bmatrix} \mathbf{a}_1 & \mathbf{a}_2 & \mathbf{a}_3 \end{bmatrix} \bar{\mathbf{m}}_2 \begin{bmatrix} \mathbf{a}_1^T \\ \mathbf{a}_2^T \\ \mathbf{a}_3^T \end{bmatrix}. \quad (33)$$

The complete decomposition is then:

$$\begin{aligned} \mathbf{M} &= \frac{1}{3}(m_1+m_2+m_3)\mathbf{I} \\ &+ m_3^*(\mathbf{a}_3\mathbf{a}_3 - \mathbf{a}_2\mathbf{a}_2) + m_1^*(\mathbf{a}_1\mathbf{a}_1 - \mathbf{a}_2\mathbf{a}_2). \end{aligned} \quad (34)$$

Double Couple - CLVD

Following Knopoff and Randall (1970) and Fitch *et al.* (1980), we can decompose a moment tensor into an isotropic part, a double couple and a compensated linear vector dipole. Let's assume again that $|m_3^*| \geq |m_2^*| \geq |m_1^*|$ in (23). We can write the deviatoric part in (23) as ($N = 1$)

$$\bar{\mathbf{m}}_1 = m_3^* \begin{bmatrix} -F & 0 & 0 \\ 0 & (F-1) & 0 \\ 0 & 0 & 1 \end{bmatrix}, \quad (35)$$

where $F = -m_1^*/m_3^*$ and $(F-1) = m_2^*/m_3^*$. Note that $0 \leq F \leq 0.5$. This constraint on F arises from the deviatoric condition $m_1^* + m_2^* + m_3^* = 0$. We can decompose (35)

into two parts representing a double couple and a CLVD

$$\bar{\mathbf{m}}_1 = m_3^* (1 - 2F) \begin{bmatrix} 0 & 0 & 0 \\ 0 & -1 & 0 \\ 0 & 0 & 1 \end{bmatrix} + m_3^* F \begin{bmatrix} -1 & 0 & 0 \\ 0 & -1 & 0 \\ 0 & 0 & 2 \end{bmatrix}, \quad (36)$$

where we assumed that the same principal stresses produce the double couple as well as the CLVD radiation. The complete decomposition (21) is then:

$$\mathbf{M} = \frac{1}{3}(m_1 + m_2 + m_3)\mathbf{I} + m_3^*(1 - 2F)(\mathbf{a}_3\mathbf{a}_3 - \mathbf{a}_2\mathbf{a}_2) \quad (37)$$

$$+ m_3^* F (2\mathbf{a}_3\mathbf{a}_3 - \mathbf{a}_2\mathbf{a}_2 - \mathbf{a}_1\mathbf{a}_1).$$

To estimate the deviation of the seismic source from the model of a pure double couple, Dziewonski *et al.* (1981) used the parameter

$$\epsilon = \left| \frac{m_{\min}^*}{m_{\max}^*} \right|, \quad (38)$$

where m_{\min}^* is the smallest eigenvalue (in the absolute sense) and m_{\max}^* is the largest (in the absolute sense), given by (24). From (35), we see that $\epsilon = F$. For a pure double couple source, $m_{\min}^* = 0$ and $\epsilon = 0$; for a pure CLVD, $\epsilon = 0.5$. Alternatively, ϵ can be expressed in percentages of CLVD (multiply ϵ by 200. The percentage of double couple is $(1 - 2\epsilon) * 100$). Dziewonski and Woodhouse (1983b, see also Giardini, 1984) investigated the variation of ϵ versus seismic moment and earthquake spatial distribution on the surface of the earth.

MOMENT TENSOR INVERSION

There are various methods of inversion for moment tensor elements. The inversion can be done in the time or frequency domain. Different data (e.g. free oscillations, surface- and body waves; different seismogram components) can be used separately or combined. In addition, certain *a priori* constraints such as $tr(\mathbf{M}) = 0$, or $M_{zz} = M_{yz} = 0$ can be imposed to stabilize the inversion, resulting in a decrease in number of resolved moment tensor elements. In this Student's Guide, we briefly outline certain approaches and refer to the original papers for further reference.

Gilbert (1970) introduced the seismic moment tensor for calculating the excitation of normal modes (Saito, 1967) of free oscillations of the earth. Gilbert (1973) suggested an inversion scheme for moment tensor elements in the frequency domain. Gilbert and Dziewonski (1975) used free oscillation data for their moment tensor inversion. Gilbert and Buland (1976) investigated on the smallest number of stations necessary for a successful inversion (see also Stump and Johnson, 1977). McCowan (1976), Mendiguren (1977), Patton and Aki (1979), Patton (1980), Romanowicz (1981), Kanamori and Given (1981, 1982), Lay *et al.* (1982), Nakanishi and Kanamori (1982, 1984), and Scott and Kanamori (1985) used long-period surface waves (typically low pass filtered at 135 sec). Stump and Johnson (1977), Strelitz (1978, 1980), Ward (1980a, b), Fitch *et al.* (1980), Langston (1981), Dziewonski *et al.* (1981), and Dziewonski and Woodhouse (1983a, b), used moment tensor inversion for body wave data (typically low pass filtered at 45 sec). A comparison between

moment tensors from surface waves and body waves was done by Fitch *et al.* (1981). Dziewonski *et al.* (1981) suggested an iterative inversion method, solving for the moment tensor elements and the centroid location (Backus and Mulcahy, 1976; Backus, 1977a; see Dziewonski and Woodhouse, 1983a for a review). The reason for that approach is that moment tensor elements trade off with the location of the earthquake. The lateral heterogeneity of the earth was considered in inversion methods by Patton (1980), Romanowicz (1981), Nakanishi and Kanamori (1982), and Dziewonski *et al.* (1984c).

The moment tensor inversion in the time domain can use the formulation in (5) (e.g. Gilbert, 1970; McCowan, 1976; Stump and Johnson, 1977; Strelitz, 1978; Fitch *et al.*, 1980; Ward, 1980b; Langston, 1981). If the source time function is not known or the assumption of a synchronous source is dropped (Sipkin, 1986), the frequency domain approach is chosen (e.g. Gilbert, 1973; Dziewonski and Gilbert, 1974; Gilbert and Dziewonski, 1975; Gilbert and Buland, 1976; Mendiguren, 1977; Stump and Johnson, 1977; Patton and Aki, 1979; Patton, 1980; Ward, 1980a, Kanamori and Given, 1981; Romanowicz, 1981):

$$d_n(\mathbf{x}, f) = M_{kj}(f) G_{nk,j}(f) \quad (39)$$

Both approaches, (5) and (39) lead to linear inversions in the time or frequency domain, respectively. The advantage of linear inversions is that a large number of fast computational algorithms are available (e.g. Lawson and Hanson, 1974; Press *et al.*, 1987). We can write either (5) or (39) in matrix form:

$$\mathbf{d} = \mathbf{G} \bar{\mathbf{m}} \quad (40)$$

In the time domain, the vector \mathbf{d} consists of n sampled values of the observed ground displacement at various arrival times, stations, and azimuths. \mathbf{G} is a $n \times 6$ matrix containing the Green's functions calculated using an appropriate algorithm and earth model, and $\bar{\mathbf{m}}$ is a vector containing the 6 moment tensor elements to be determined (Stump and Johnson, 1977). In the frequency domain, (40) can be written separately for each frequency. \mathbf{d} consists of real and imaginary parts of the displacement spectra. Weighting can be introduced which actually smoothes the observed spectra subjectively (Mendiguren, 1977; see also Ward, 1980b for weighting of body-wave data in the time domain). In the same way, \mathbf{G} and $\bar{\mathbf{m}}$ contain real and imaginary parts. $\bar{\mathbf{m}}$ contains also the transform of the source time function of each moment tensor element. If constraints are applied to the inversion, then $\bar{\mathbf{m}}$ can contain a smaller number of moment tensor elements. In such a case, \mathbf{G} has to be changed accordingly. We refer to Aki and Richards (1980) for the details of solving (40) for $\bar{\mathbf{m}}$ (Note that (40) is identical to their (12.83)).

The following presents an outline of the processing steps in a moment tensor inversion. The first step is the data acquisition and the preprocessing. We need data with good signal to noise ratio that are unclipped and that have a good coverage of the focal sphere (Satake, 1985). Glitches (non-seismic high amplitude spikes due to non-linearity of instruments e.g. Dziewonski *et al.*, 1981) have to be identified and possibly removed. Analog data have to be digitized. The effect of non-orthogonality of the analog recorder must be corrected. The digitized

record has to be interpolated and resampled with a constant sampling rate. At this point, a comparison of the sampled waveform with the original one can help to identify digitization errors. The horizontal components will be rotated into radial and transverse components. Linear trends have to be identified and removed. The instrument effect is considered next (for WWSSN data see Hagiwara, 1958; for SRO data see McCowan and Lacoss, 1978; for IDA data see Agnew *et al.*, 1976). We can use either one of the two approaches: i) we can remove the instrument effect from the observed data and compare with theory or ii) we can apply the instrument response to the synthetic Green's functions and compare with observed data. The nominal instrument response can be used or the calibration of the instrument can be checked by using f.e. the calibration pulse on the record. In addition, the polarity of the instruments should be verified, e.g. from records of known nuclear explosions. High frequency noise in the data is removed by low-pass filtering. Amplitudes are corrected for geometrical spreading and reflections at the free surface of the earth (Bullen and Bolt, 1985). For surface waves, the moving window analysis (Landisman *et al.*, 1969) is applied in order to determine the group velocity dispersion. From this analysis, we can identify the fundamental mode Rayleigh and Love waves which can then be isolated.

Second, synthetic Green's functions are calculated. Notice that the Green's functions are dependent on the earth-model, the location of the point source (centroid of the stress glut, or epicenter and focal depth), and the receiver position.

The third step is the proper inversion, i.e. the solution of (40) (Aki and Richards, 1980). Usually, the inversion is formulated as least squares problem (Gilbert, 1973; Gilbert and Buland, 1976; Mendiguren, 1977; Stump and Johnson, 1977). However, using other norms can have advantages in situations where less sensitivity to gross errors like polarity reversions is required (Claerbout and Muir, 1973; Fitch *et al.*, 1980; Patton, 1980).

The source time function in (5) is often assumed to be a step function (Gilbert, 1970, 1973; McCowan, 1976; Stump and Johnson, 1977; Patton and Aki, 1979; Patton, 1980; Ward, 1980b; Dziewonski *et al.*, 1981; Kanamori and Given, 1981). Aiming at the recovery of source time functions, Burdick and Mellman (1976) used a powerful iterative waveform inversion method based on optimizing the cross-correlation between observed, long-period body-wave trains and synthetics. The same approach was used by Wallace *et al.*, (1981) in-order to invert for fault plane solutions. Other methods were employed by Strelitz (1980) and Kikuchi and Kanamori (1982) for large earthquakes (see also Lundgren *et al.*, 1988). Christensen and Ruff (1985) reported on a trade-off between source time function and source depth for shallow events.

If the focal depth is not known, then a linear inversion can be done for each depth out of a number of trial depths. The most probable depth will minimize the quadratic error between observed and theoretical waveforms (Mendiguren, 1977; Patton and Aki, 1979; Patton, 1980; Romanowicz, 1981). The influence of source depth on the results of the moment tensor inversion was investigated by Sipkin (1982; Dziewonski *et al.*, 1987b). Differences in source depth influence the relative excitation of normal

modes, causing systematic errors in the inversion.

Systematic errors in the inversion are also due to deviations of the earth-model from the actual properties of the earth, affecting the synthetic Green's functions. This is a fundamental problem in the sense that we are able to separate the source effect from the observed seismogram only to a limited accuracy (Mendiguren, 1977; Langston, 1981; Silver and Jordan, 1982; O'Connell and Johnson, 1988). A major problem is the effect of lateral heterogeneity of the earth (Engdahl and Kanamori, 1980; Romanowicz, 1981; Gombert and Masters, 1988; Snieder and Romanowicz, 1988). For example, a relative change of 0.5 % due to lateral heterogeneity can cause a mislocation in the order of of 50 km at epicentral distances of about 90 degrees (Dziewonski and Woodhouse, 1983b). Giardini (1984) and Ekström and Dziewonski (1985) reported on regional shifts in centroid positions due to lateral heterogeneity. In the inversion, lateral heterogeneity is often neglected, i.e. the calculation of the Green's functions is usually based on parallel layers of lateral homogeneity (Harkrider, 1964, 1970; Langston and Helmberger, 1975; Harkrider, 1976). Nakanishi and Kanamori (1982) included the effect of lateral heterogeneity into the moment tensor inversion. Another approach was developed for earthquakes within a small source area: a calibration event is declared (mechanism known); the spectral ratio of any earthquake in that region and the calibration event will result in isolating the difference in source effects - the influence of the path is eliminated (Patton, 1980). It seems that the errors due to lateral heterogeneity are usually large enough to make a statistical significant detection of an isotropic component of the moment tensor difficult (Okal and Geller, 1979; Silver and Jordan, 1982; Vasco and Johnson, 1988).

Patton and Aki (1979) investigated the influence of noise on the inversion of long-period surface wave data. They found that additive noise such as background recording noise does not severely affect the results of a linear inversion. However, multiplicative noise (signal generated noise) caused by focusing, defocusing, multipathing, higher mode or body wave interference, and scattering distorts the inversion results significantly (overestimation or underestimation of moment tensor elements, deviation from the source mechanism; Patton, 1980; Ward, 1980b). Finally, body waves of events with moments larger than 10^{27} dyne-cm are severely affected by finiteness of the source and directivity. If not corrected for, an inversion can lead to severe errors in the moment tensor elements (Dziewonski *et al.*, 1981; Kanamori and Given, 1981; Patton and Aki, 1979; Lay *et al.*, 1982; Giardini, 1984).

The inversion has only a limited resolution of moment tensor elements for certain data. If we have spectra of fundamental mode Rayleigh waves only, the constraint that the trace of the moment tensor vanishes (no volume change) must be applied (Mendiguren, 1977; Patton and Aki, 1979). This constraint is linear. Another constraint which is often applied in addition is that one eigenvalue vanishes (approximating the source by a double couple). This constraint is not linear (Strelitz, 1978; Ward, 1980b). In such a case, the inversion is iterative, using a linearized version of the constraints (Ward, 1980b). For earthquakes at shallow depths (less than

A Student's Guide to and Review of Moment Tensors

about 30 km), the moment tensor elements M_{zz} and M_{yz} corresponding to vertical dip slip faulting are not well constrained from long-period surface wave data since the related excitation functions assume very small values near the surface of the earth (Fitch *et al.*, 1981; Dziewonski *et al.*, 1981; Kanamori and Given, 1981, 1982; Dziewonski and Woodhouse, 1983a). In order to overcome this problem, additional independent data, such as fault strike (observed surface breakage) can be introduced into the inversion. Another approach is to constrain these moment tensor elements to be zero. Thus, possible fault mechanisms are restricted to vertical strike slip or 45 degree dip slip (Kanamori and Given, 1981, 1982).

In Appendix V, we relate the Green's functions in the formulation of Herrmann and Wang (1985) to a simple moment tensor inversion scheme. This inversion example is aimed at testing computer programs.

CONCLUSION

A seismic moment tensor describes the equivalent forces of a seismic point source. The eigenvectors are the principal axes of the seismic moment tensor. For pure double couple sources, the principal axis corresponding to the negative eigenvalue is the pressure axis, the principal axis corresponding to the positive eigenvalue is the tension axis, and the principal axis corresponding to the eigenvalue zero gives the null axis. The pressure, tension, and null axes can be displayed in the familiar focal mechanism plot (fault plane solution). For general seismic sources, we can decompose the seismic moment tensor. First, we can separate out the isotropic component which describes the volume change in the source. The leftover part of the moment tensor has, in general, three nonvanishing eigenvalues. This deviatoric part of the moment tensor can be decomposed into a number of simple combinations of equivalent forces. Obviously, there is no unique moment tensor decomposition, i.e. unique model of equivalent forces. We outlined methods of determining moment tensor elements from observations, indicating that recording noise as well as systematic errors due to an insufficient knowledge of the Green's functions can introduce errors into the moment tensor elements. This suggests caution when apparent non-double couple sources result from the inversion.

Randall and Knopoff (1970), Gilbert and Dziewonski (1975), Dziewonski *et al.* (1981), Kanamori and Given (1981, 1982), Dziewonski and Woodhouse (1983b), Giardini (1984), and Scott and Kanamori (1985) reported that some seismic sources cannot be described by a pure double couple. One explanation is that some fault planes show a complex geometry (Dziewonski and Woodhouse, 1983b). Another explanation can be that some sources deviate from the model of a sudden shear dislocation; they can be due to a rapidly propagating phase transition (Knopoff and Randall, 1970; Dziewonski and Woodhouse, 1983b). However, the simple inversion experiment in Appendix V pointed out that the deviation from a pure double couple can also be due to the presence of noise in the data (Stump and Johnson, 1977; Patton and Aki, 1979; Patton, 1980; Ward, 1980b; Wallace, 1985; O'Connell and Johnson, 1988).

ACKNOWLEDGMENTS

We thank two anonymous reviewers for their helpful criticism of the manuscript. Critical remarks by Ozgur Mindevalli are appreciated. Funds for this research were provided by the Defense Advanced Research Projects Agency under contract F49628-87-K-0047 monitored by the Air Force Geophysics Laboratory.

APPENDIX I

In the following, we give some mathematical definitions of tensors, the eigenvalue problem and dyadics following Arfken (1985).

Let \mathbf{M} be a moment tensor of second rank (order). Then, \mathbf{M} is represented as a 3×3 matrix in a given reference frame. Let a_{pk} be the cosine of the angle between the p axis of another coordinate system and the k axis. Then the components of \mathbf{M} , M_{kj} , transform into the new reference frame by the relation

$$M_{pq} = a_{kp} a_{jq} M_{kj} \quad , \quad (\text{A1.1})$$

where we need to sum over repeated indices (summation convention).

Given a moment tensor \mathbf{M} , let's assume that there is a vector \mathbf{a} and a scalar m such that

$$\mathbf{M} \mathbf{a} = m \mathbf{a} \quad . \quad (\text{A1.2})$$

\mathbf{a} is called eigenvector of \mathbf{M} and m is the corresponding eigenvalue. For calculating the eigenvalues and eigenvectors of a given moment tensor (solving the eigenvalue problem), we transform (A1.2)

$$(\mathbf{M} - m \mathbf{I}) \mathbf{a} = 0 \quad , \quad (\text{A1.3})$$

where \mathbf{I} is the identity matrix. (A1.3) is a system of 3 simultaneous homogeneous linear equations in a_k . Non-trivial solutions are found by solving the secular equation (characteristic polynomial)

$$\det(\mathbf{M} - m \mathbf{I}) = 0 \quad , \quad (\text{A1.4})$$

where "det" means the determinant. (A1.4) is a polynomial of third degree. It has three real roots, i.e. eigenvalues, since the moment tensor is real and symmetric (Faddeeva, 1959). Substituting each eigenvalue m_i into (A1.3) gives the corresponding eigenvector \mathbf{a}_i . The eigenvectors are orthogonal. Multiplying each eigenvector by its inverse norm, we get the orthonormal eigenvectors, renaming them as \mathbf{a}_i :

$$\mathbf{a}_i \mathbf{a}_j = \delta_{ij} \quad . \quad (\text{A1.5})$$

Knowing the eigenvectors, we can diagonalize \mathbf{M} (principal axis transformation). Let \mathbf{A} be the matrix whose columns are the orthonormal eigenvectors of \mathbf{M} . From (A1.5), we see that \mathbf{A} is orthogonal: $\mathbf{A}^T = \mathbf{A}^{-1}$. Then, $\mathbf{A}^T \mathbf{M} \mathbf{A} = \mathbf{m}$, where \mathbf{m} is diagonal, consisting of the eigenvalues of \mathbf{M} .

We represent a dyadic by writing two vectors \mathbf{a} and \mathbf{b} together as \mathbf{ab} (see Appendix A in Ben-Menahem and Singh, 1981). These two vectors forming the dyadic are not operating on each other, but define a 3×3 matrix. Let \mathbf{i} , \mathbf{j} , and \mathbf{k} be unit vectors along a right handed Cartesian coordinate system. The dyadic \mathbf{ab} is defined as

$$\begin{aligned}
 \mathbf{ab} &= (a_x \mathbf{i} + a_y \mathbf{j} + a_z \mathbf{k}) (b_x \mathbf{i} + b_y \mathbf{j} + b_z \mathbf{k}) \\
 &= \mathbf{ii} a_x b_x + \mathbf{ij} a_x b_y + \mathbf{ik} a_x b_z \\
 &+ \mathbf{ji} a_y b_x + \mathbf{jj} a_y b_y + \mathbf{jk} a_y b_z \\
 &+ \mathbf{ki} a_z b_x + \mathbf{kj} a_z b_y + \mathbf{kk} a_z b_z \\
 &= \begin{bmatrix} a_x b_x & a_x b_y & a_x b_z \\ a_y b_x & a_y b_y & a_y b_z \\ a_z b_x & a_z b_y & a_z b_z \end{bmatrix}.
 \end{aligned} \tag{A1.6}$$

For $\mathbf{a} = \mathbf{b}$, we get (26). The multiplication of a vector \mathbf{c} from the left is

$$\mathbf{c} \cdot \mathbf{ij} = [(\mathbf{ic}_x + \mathbf{jc}_y + \mathbf{kc}_z) \cdot \mathbf{ij}] = c_x \mathbf{j} \tag{A1.7}$$

If the dyadic is symmetric, the multiplication of any vector with the dyadic is commutative, i.e. $\mathbf{ab} = \mathbf{ba}$. In general, we can understand a dyadic as a tensor of second rank. By a proper choice of the coordinate system, a symmetric dyadic can always be transformed into diagonal form (principal axis transformation). As an example, we can rewrite (10) using dyadics (Gilbert, 1973):

$$\begin{aligned}
 \mathbf{u}\nu + \nu\mathbf{u} &= \mathbf{tt} - \mathbf{pp} \\
 &= 0.5 [(\mathbf{t}+\mathbf{p})(\mathbf{t}-\mathbf{p}) + (\mathbf{t}-\mathbf{p})(\mathbf{t}+\mathbf{p})].
 \end{aligned} \tag{A1.8}$$

APPENDIX II

The PDE monthly listings (NEIS) routinely publish centroid moment tensor solutions in the notation of the normal mode theory following Dziewonski *et al.* (1981). For reference, the spherical moment tensor elements, f_i , in the notation of Gilbert and Dziewonski (1975), Dziewonski *et al.* (1981), and Dziewonski and Woodhouse (1983a) are compared to the moment tensor elements as given in (18) following Aki and Richards (1980).

$$\begin{aligned}
 f_1 &= M_{rr} = M_{zz} \\
 f_2 &= M_{\Theta\Theta} = M_{xx} \\
 f_3 &= M_{\phi\phi} = M_{yy} \\
 f_4 &= M_{r\Theta} = M_{xz} \\
 f_5 &= M_{r\phi} = -M_{yz} \\
 f_6 &= M_{\Theta\phi} = -M_{xy},
 \end{aligned} \tag{A2.1}$$

where (r, Θ, ϕ) are the geographical coordinates at the source. Θ is the colatitude ($\Theta = 0$ at the north pole) and ϕ is the longitude of the point source. The sign of the off-diagonal moment tensor elements depend on the orientation of the coordinate system (Fitch *et al.*, 1981). But the eigenvalues and the eigenvectors of the moment tensor in the formulation of (18) or (A2.1) are identical, which can be shown by comparing the solutions to the secular equation (Appendix I). This result is expected since physical laws should not depend on the choice of the reference frame. The slip vector \mathbf{u} and fault normal ν are (Dziewonski and Woodhouse, 1983a)

$$\begin{aligned}
 \mathbf{u} &= \bar{u} (-\cos \lambda \cos \Phi - \cos \delta \sin \lambda \sin \Phi) \mathbf{e}_\Theta \\
 &+ \bar{u} (\cos \lambda \sin \Phi - \cos \delta \sin \lambda \cos \Phi) \mathbf{e}_\phi \\
 &+ \bar{u} \sin \lambda \sin \delta \mathbf{e}_r,
 \end{aligned} \tag{A2.2}$$

and

$$\nu = \sin \delta \sin \Phi \mathbf{e}_\Theta + \sin \delta \cos \Phi \mathbf{e}_\phi + \cos \delta \mathbf{e}_r. \tag{A2.3}$$

These two equations are identical to (4.122) in Ben-Menahem and Singh (1981). The differences in sign compared to (15) and (16) can be fully explained by noting that $\mathbf{e}_r = -\mathbf{e}_z$, $\mathbf{e}_\phi = \mathbf{e}_y$, and $\mathbf{e}_\Theta = -\mathbf{e}_x$; in other words, \mathbf{e}_Θ , \mathbf{e}_ϕ , and \mathbf{e}_r are unit vectors towards south, east, and up, respectively (defining a right handed system).

APPENDIX III

In order to gain some experience in the relationships between a moment tensor and a fault plane solution, three simple focal mechanisms are discussed in detail. These will be vertical strike slip, 45 degree dip slip, and vertical dip slip faults. These three fault plane solutions form a complete set: The seismic radiation from a dislocation on a plane dipping an arbitrary angle (but striking north-south) can be expressed as a linear combination of these three solutions (Burridge *et al.*, 1964; Ben-Menahem and Singh, 1968).

Vertical strike slip fault

The following focal mechanism is assumed: (strike) $\Phi = 0^\circ$, (dip) $\delta = 90^\circ$, and (slip) $\lambda = 0^\circ$. From (15) and (16), the slip vector on the fault plane is $\mathbf{u} = (1, 0, 0)$ and the vector normal to the fault plane is $\nu = (0, 1, 0)$. The moment tensor can be determined from (18).

$$\mathbf{M} = \begin{bmatrix} 0 & M_0 & 0 \\ M_0 & 0 & 0 \\ 0 & 0 & 0 \end{bmatrix}. \tag{A3.1}$$

The eigenvalues and eigenvectors of this tensor (Example 4.6.1 in Arfken, 1985, see also Appendix I) are shown in Table A.1 (The components of the eigenvectors are north, east, and down).

TABLE A.1

EIGENVALUE	EIGENVECTOR
0	(0.0000, 0.0000, -1.0000)
M_0	(0.7071, 0.7071, 0.0000)
$-M_0$	(-0.7071, 0.7071, 0.0000)

The eigenvector \mathbf{b} corresponding to the eigenvalue zero is the null-axis, the eigenvector \mathbf{t} corresponding to the positive eigenvalue gives the tension axis, T, and the eigenvector \mathbf{p} corresponding to the negative eigenvalue gives the pressure axis, P, of a focal mechanism.

The focal mechanism is obtained by using (7)-(14) (Herrmann, 1975). For the trend and plunge (in degrees) of the X-, Y-, null-, T-, and P-axes, we get (90, 0), (180, 0), (270, 90), (45, 0), and (135, 0), respectively. The trend of both the P and T axes can be shifted by 180° (Figure A.1a); i.e. the P-axis can also be described by $(315^\circ, 0^\circ)$ and the T-axis by $(225^\circ, 0^\circ)$. This ambiguity can be followed through to the moment tensor: The sign of an eigenvector is not constrained by the solution of the eigenvalue problem (Arfken, 1985). However, any choice of sign leads to the same focal mechanism.

A Student's Guide to and Review of Moment Tensors

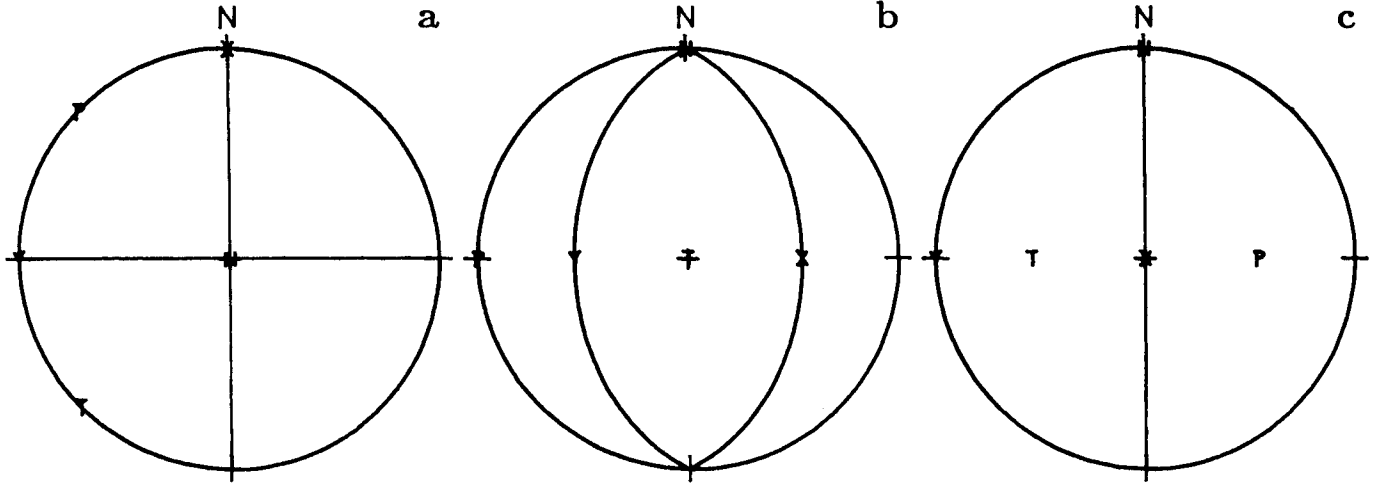


Fig. A.1. Focal mechanisms of a vertical strike slip fault (strike = 0°, dip = 90°, slip = 0°), (a), a 45 degree dip slip fault (strike = 0°, dip = 45°, slip = 90°), (b), and a vertical dip slip fault (strike = 0°, dip = 90°, slip = 90°), (c) (Appendix III).

45 degree dip slip fault

The following focal mechanism is assumed: (strike) $\Phi = 0^\circ$, (dip) $\delta = 45^\circ$, and (slip) $\lambda = 90^\circ$. From (15) and (16), $\mathbf{u} = (0, -0.7071, -0.7071)$ and $\mathbf{v} = (0, 0.7071, -0.7071)$. The moment tensor is calculated from (18).

$$\mathbf{M} = \begin{bmatrix} 0 & 0 & 0 \\ 0 & -M_0 & 0 \\ 0 & 0 & M_0 \end{bmatrix} \quad (\text{A3.2})$$

The corresponding eigenvalues and eigenvectors are shown in Table A.2.

TABLE A.2

EIGENVALUE	EIGENVECTOR
0	(-1, 0, 0)
M_0	(0, 0, -1)
$-M_0$	(0, 1, 0)

The fault plane solution is obtained from (7)-(14) (Herrmann, 1975). For the trend and plunge (in degrees) of the X-, Y-, null-, T-, and P-axes, we get (90, 45), (270, 45), (360, 0), (180, 90), and (270, 0), respectively. The trend of the P and null axes can be shifted by 180° (Figure A.1b) to (90°, 0°) and (180°, 0°), respectively.

Vertical dip slip fault

The following focal mechanism is assumed: (strike) $\Phi = 0^\circ$, (dip) $\delta = 90^\circ$, and (slip) $\lambda = 90^\circ$. From (15) and (16), $\mathbf{u} = (0, 0, -1)$ and $\mathbf{v} = (0, 1, 0)$. The moment tensor is calculated from (18).

$$\mathbf{M} = \begin{bmatrix} 0 & 0 & 0 \\ 0 & 0 & -M_0 \\ 0 & -M_0 & 0 \end{bmatrix} \quad (\text{A3.3})$$

The corresponding eigenvalues and eigenvectors are shown in Table A.3.

TABLE A.3

EIGENVALUE	EIGENVECTOR
0	(-1.0000, 0.0000, 0.0000)
M_0	(0.0000, 0.7071, -0.7071)
$-M_0$	(0.0000, 0.7071, 0.7071)

The fault plane solution is obtained from (7)-(14) (Herrmann, 1975). For the trend and plunge (in degrees) of the X-, Y-, null-, T-, and P-axes, we get (0, 90), (90, 0), (180, 0), (270, 45), and (90, 45), respectively. The trend of the null axis can be shifted by 180° (Figure A.1c) to (360°, 0°).

APPENDIX IV

In the following, examples of the five methods of moment tensor decomposition are presented.

In order to construct a moment tensor that *does not* lead to a simple double couple mechanism, let

$$\mathbf{M}_1 = 1 \begin{bmatrix} 1 & 0 & 0 \\ 0 & 1 & 0 \\ 0 & 0 & 1 \end{bmatrix} \quad (\text{A4.1})$$

$$\mathbf{M}_2 = 6 \begin{bmatrix} 0 & 1 & 0 \\ 1 & 0 & 0 \\ 0 & 0 & 0 \end{bmatrix} \quad (\text{A4.2})$$

$$\mathbf{M}_3 = 3 \begin{bmatrix} 0 & 0 & 0 \\ 0 & -1 & 0 \\ 0 & 0 & 1 \end{bmatrix} \quad (\text{A4.3})$$

$$\mathbf{M}_4 = 1 \begin{bmatrix} 0 & 0 & 0 \\ 0 & 0 & -1 \\ 0 & -1 & 0 \end{bmatrix} \quad (\text{A4.4})$$

The first moment tensor represents an explosion, the others are the familiar ones from Appendix III, representing a vertical strike-slip, a 45 degree dip-slip, and a vertical dip-slip fault, respectively. All four moment tensors are superimposed in order to describe a complex source that is dominated by a vertical strike slip mechanism.

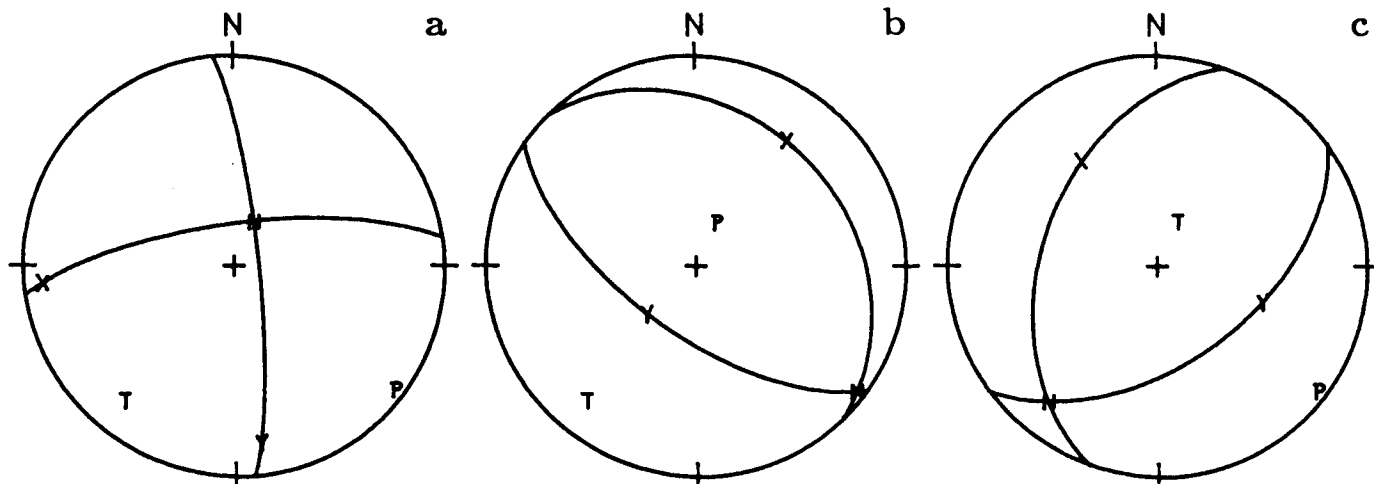


Fig. A.2. Focal mechanisms of the double couples from the moment tensor decomposition (Appendix IV). (a) major couple of the moment tensor in (A4.5), elementary moment tensor EMT3 in (A4.6), and second term on the RHS of (A4.9) (strike = 355° , dip = 80° , slip = 16°), (b) elementary moment tensor EMT2 in (A4.6) (strike = 125° , dip = 63° , slip = -95°), (c) elementary moment tensor EMT4 in (A4.6) (strike = 199° , dip = 44° , slip = 63°).

The result is

$$\mathbf{M} = \begin{bmatrix} 1 & 6 & 0 \\ 6 & -2 & -1 \\ 0 & -1 & 4 \end{bmatrix}. \quad (\text{A4.5})$$

Table A.4 shows the eigenvalues of (A4.5) and the corresponding eigenvectors, which are the principal axes of \mathbf{M} .

TABLE A.4

EIGENVALUE	EIGENVECTOR
3.8523	(-0.2938, -0.1397, -0.9456)
5.8904	(0.7352, 0.5992, -0.3170)
-6.7427	(0.6109, -0.7883, -0.0734)

The sum of the eigenvalues is equal to 3, which is the expected value for the sum of the eigenvalues of (A4.1), describing an explosion.

In order to calculate the deviatoric part of the given moment tensor, the isotropic part is removed by subtracting one third of the trace of (A4.5) from each diagonal element. The solution to the corresponding eigenvalue problem leads to the same eigenvectors as above. This indicates that the principal axes of the complete moment tensor are the same as the principal axes of the corresponding deviatoric tensor. The deviatoric eigenvalues are 2.8523, 4.8904, and -7.7427 in the order of Table A.4 (see (24)). From (38), $\epsilon = 0.37$, i.e. the given moment tensor has a double couple component of 26 % and a CLVD component of 74 %.

For the determination of the *major couple* from (32), we identify the eigenvector (0.6109, -0.7883, -0.0734) corresponding to the deviatoric eigenvalue of -7.7 as the P-axis, the eigenvector (0.7352, 0.5992, -0.3170) corresponding to the eigenvalue of 4.9 as the T-axis, and

the eigenvector (-0.2938, -0.1397, -0.9456) with eigenvalue 2.9 as the null-axis. The fault plane solution of the major double couple gives for the X-, Y-, null-, T-, and P-axes (in degrees): (172, 16), (265, 10), (25, 71), (219, 18), and (128, 4), respectively (Figure A.2a). The major double couple gives a good estimate of the major contribution to the faulting which is predominantly strike slip (compare Figures A.1a and A.2a).

Next, the moment tensor in (A4.5) is decomposed into an isotropic part and three double couples following (29) which is evaluated by using (26) together with the data in Table A.4. The numbering of the eigenvalues and eigenvectors in (29) follows the columns of Table A.4, but that is not relevant to the solution. The calculation gives

$$\begin{aligned} \mathbf{M} = & 1 \begin{bmatrix} 1 & 0 & 0 \\ 0 & 1 & 0 \\ 0 & 0 & 1 \end{bmatrix} + 0.6794 \begin{bmatrix} 0.4542 & 0.3995 & -0.5109 \\ 0.3995 & 0.3396 & -0.3220 \\ -0.5109 & -0.3220 & -0.7936 \end{bmatrix} \\ & + 4.2110 \begin{bmatrix} 0.1673 & 0.9221 & -0.1882 \\ 0.9221 & -0.2623 & -0.2477 \\ -0.1882 & -0.2477 & 0.0951 \end{bmatrix} \\ & + 3.5316 \begin{bmatrix} -0.2869 & 0.5226 & 0.3227 \\ 0.5226 & -0.6019 & 0.0743 \\ 0.3227 & 0.0743 & 0.8887 \end{bmatrix}. \quad (\text{A4.6}) \end{aligned}$$

This equation is identical to (A4.5). The first elementary moment tensor (EMT1) on the RHS of (A4.6) describes the explosion (isotropic component of (A4.5)) and is identical to (A4.1). The last three elementary moment tensors on the RHS (EMT2, EMT3, EMT4, respectively) represent pure double couple sources since the eigenvalues of each tensor is 0 and ± 1 . The three elementary moment tensors have identical eigenvectors which are the same vectors as shown in Table A.4. However, the correlation between eigenvector and eigenvalue (i.e. null-, P-, and T-axes) varies. Note that replac-

A Student's Guide to and Review of Moment Tensors

ing M_{kj} by $-M_{kj}$ switches the sign of the eigenvalues (leaving the eigenvectors untouched), which is identical to interchanging the P- and T-axes.

From the eigenvalues and the eigenvectors, the fault plane solution for each elementary moment tensor is determined and shown in Table A.5.

TABLE A.5

AXIS	EMT2	EMT2	EMT3	EMT3	EMT4	EMT4
	TRD	PLG	TRD	PLG	TRD	PLG
	(deg.)	(deg.)	(deg.)	(deg.)	(deg.)	(deg.)
X	36	26	172	16	324	38
Y	226	63	265	10	109	46
NULL	128	4	25	71	219	18
T	219	18	219	18	25	71
P	25	71	128	4	128	4

The focal mechanisms corresponding to EMT2 - EMT4 are shown in Figures A.2b, A.2a, and A.2c, respectively. Note that the positions of the axes remain fixed in these figures, where only the correlation to the eigenvalues changes. The fault plane solution representing the third elementary moment tensor EMT3 in (A4.6) is identical to the fault plane solution of the major couple (Figure A.2a). Notice that this solution has also the largest coefficient in (A4.6). This solution is an approximation to the major contributor of the moment tensor (Figure A.1a and (A4.2)). However, the other fault plane solutions (Figure A.2b and A.2c) do not show similarities to the input fault mechanisms (Figure A.1b and A.1c).

The seismic moments of the elementary moment tensors are given by the coefficients in (A4.6). The sum of the seismic moments of the elementary moment tensors is 1.4 times larger than the seismic moment of the composite moment tensor in (A4.5).

Next, the moment tensor in equation (A4.5) is decomposed into an isotropic part and three vector dipoles following (27) which is evaluated by using (26) together with Table A.4.

$$\begin{aligned}
 \mathbf{M} = & \mathbf{1} \begin{bmatrix} 1 & 0 & 0 \\ 0 & 1 & 0 \\ 0 & 0 & 1 \end{bmatrix} + 2.8523 \begin{bmatrix} 0.0863 & 0.0410 & 0.2779 \\ 0.0410 & 0.0195 & 0.1321 \\ 0.2779 & 0.1321 & 0.8941 \end{bmatrix} \\
 & + 4.8904 \begin{bmatrix} 0.5405 & 0.4405 & -0.2330 \\ 0.4405 & 0.3591 & -0.1899 \\ -0.2330 & -0.1899 & 0.1005 \end{bmatrix} \\
 & - 7.7427 \begin{bmatrix} 0.3732 & -0.4816 & -0.0448 \\ -0.4816 & 0.6214 & 0.0578 \\ -0.0448 & 0.0578 & 0.0054 \end{bmatrix}. \tag{A4.7}
 \end{aligned}$$

This equation is identical to (A4.5). In the notation used above, each of the elementary moment tensors EMT2, EMT3, and EMT4 have two eigenvalues equal to zero, the third one equals one. EMT2 is represented by the eigenvector (0.2938, 0.1397, 0.9456), EMT3 by (-0.7352, -0.5992, 0.3170), and EMT4 by (0.6109, -0.7883, -0.0734). These vector dipoles are mutually orthonormal. Notice that these vector dipoles are identical to the eigenvectors of equation (A4.5), which are the principal axes of the tensor (Table A.4). EMT2 represents the null-, EMT3 the tension-, and EMT4 the pressure axis. The seismic

moments of the elementary moment tensors are given by the coefficients in (A4.7) which are identical to the deviatoric eigenvalues of (A4.5). This exercise demonstrated that vector dipoles are related to the eigenvectors scaled by the corresponding eigenvalue of a given moment tensor, which makes an evaluation of (A4.7) obsolete.

Alternatively, the moment tensor in equation (A4.5) can be decomposed into an isotropic part and three compensated linear vector dipoles using (30).

$$\begin{aligned}
 \mathbf{M} = & \mathbf{1} \begin{bmatrix} 1 & 0 & 0 \\ 0 & 1 & 0 \\ 0 & 0 & 1 \end{bmatrix} + 1.2841 \begin{bmatrix} -0.7411 & 0.1231 & 0.8336 \\ 0.1231 & -0.9415 & 0.3963 \\ 0.8336 & 0.3963 & 1.6823 \end{bmatrix} \\
 & + 1.9635 \begin{bmatrix} 0.6215 & 1.3216 & -0.6991 \\ 1.3216 & 0.0773 & -0.5697 \\ -0.6991 & -0.5697 & -0.6985 \end{bmatrix} \\
 & - 2.2476 \begin{bmatrix} 0.1196 & -1.4447 & -0.1345 \\ -1.4447 & 0.8642 & 0.1734 \\ -0.1345 & 0.1734 & -0.9838 \end{bmatrix}. \tag{A4.8}
 \end{aligned}$$

This equation is identical to (A4.5). The seismic moments of the elementary moment tensors are given by the product of the respective coefficient and $\sqrt{3}$. The eigenvalues and eigenvectors for (A4.8) are shown in Table A.6, using the same notation as above. Note that the eigenvectors are identical to those in Table A.4.

TABLE A.6

EMT	EIGENVALUE	EIGENVECTOR
2	-1	(0.6109, -0.7883, -0.0734)
	-1	(0.7352, 0.5992, -0.3170)
	2	(-0.2938, -0.1397, -0.9456)
3	-1	(-0.2938, -0.1397, -0.9456)
	-1	(0.6109, -0.7883, -0.0734)
	2	(0.7352, 0.5992, -0.3170)
4	-1	(0.7352, 0.5992, -0.3170)
	-1	(-0.2938, -0.1397, -0.9456)
	2	(0.6109, -0.7883, -0.0734)

Next, the moment tensor in (A4.5) is decomposed into an isotropic part, a double couple and CLVD following (37), where $\epsilon = F = 0.3684$.

$$\begin{aligned}
 \mathbf{M} = & \mathbf{1} \begin{bmatrix} 1 & 0 & 0 \\ 0 & 1 & 0 \\ 0 & 0 & 1 \end{bmatrix} + 2.0379 \begin{bmatrix} 0.1673 & 0.9221 & -0.1882 \\ 0.9221 & -0.2623 & -0.2477 \\ -0.1882 & -0.2477 & 0.0951 \end{bmatrix} \\
 & - 2.8523 \begin{bmatrix} 0.1196 & -1.4447 & -0.1345 \\ -1.4447 & 0.8642 & 0.1734 \\ -0.1345 & 0.1734 & -0.9838 \end{bmatrix}. \tag{A4.9}
 \end{aligned}$$

This equation is identical to (A4.5). Notice that the second term on the RHS corresponds to EMT3 in (A4.6) and to the *major* double couple. These three tensors all have the same fault plane solution (Figure A.2a). The third term in (A4.9) corresponds to EMT4 in (A4.8), representing a CLVD (see Table A.6).

As final remark, let's consider the decomposition equations (27), (29), and (30) for a simple double couple source ($\epsilon = 0$), e.g. let $m_1 = -m_2 = 1$, and $m_3 = 0$. Then, $\mathbf{M} = \mathbf{a}_1 \mathbf{a}_1 - \mathbf{a}_2 \mathbf{a}_2$ for all three equations. That is, we get one pure double couple out of the decomposition. For a CLVD ($\epsilon = 0.5$), let's assume that $m_1 = m_2 = -1$,

and $m_3 = 2$. Then all three formulas give $\mathbf{M} = 2 \mathbf{a}_3 \mathbf{a}_3 - \mathbf{a}_1 \mathbf{a}_1 - \mathbf{a}_2 \mathbf{a}_2$, representing one CLVD.

APPENDIX V

In this section, we relate the Green's functions in the formulation of Herrmann and Wang (1985) to a moment tensor inversion scheme. Following the theory given by Herrmann and Wang (1985), the Fourier transformed displacements at the free surface at the distance r from the origin due to an arbitrarily oriented double couple without moment is

$$\begin{aligned} d_z(r, z=0, \omega) &= ZSS A_1 + ZDS A_2 + ZDD A_3 \\ d_r(r, z=0, \omega) &= RSS A_1 + RDS A_2 + RDD A_3 \\ d_\phi(r, z=0, \omega) &= TSS A_4 + TDS A_5 \end{aligned} \quad (\text{A5.1})$$

where d_z is the vertical displacement (positive upward), d_r is the radial displacement, and d_ϕ is the tangential displacement (positive in a direction clockwise from north). The functions ZSS, ZDS, ZDD, RSS, RDS, RDD, TSS, and TDS together with ZEP and REP are the ten Green's functions required to calculate a wave field due to an arbitrary point dislocation source or point explosion buried in a plane layered medium (Wang and Herrmann, 1980; Herrmann and Wang, 1985). As before, let $\mathbf{u}=(u_x, u_y, u_z)$ and $\boldsymbol{\nu}=(\nu_x, \nu_y, \nu_z)$ be the dislocation vector and vector normal to the fault plane, respectively. Note that (15) and (16) are identical to the formulation used by Herrmann and Wang (1985), where our \mathbf{u} equals their \mathbf{f} and our $\boldsymbol{\nu}$ equals their \mathbf{n} (1 = x-axis, 2 = y-axis, 3 = z-axis). Then

$$\begin{aligned} A_1 &= (u_x \nu_x - u_y \nu_y) \cos(2az) + (u_x \nu_y + u_y \nu_x) \sin(2az) \\ A_2 &= (u_x \nu_z + u_z \nu_x) \cos(az) + (u_y \nu_z + u_z \nu_y) \sin(az) \\ A_3 &= u_z \nu_z \end{aligned} \quad (\text{A5.2})$$

$$\begin{aligned} A_4 &= (u_x \nu_x - u_y \nu_y) \sin(2az) - (u_x \nu_y + u_y \nu_x) \cos(2az) \\ A_5 &= (u_x \nu_z + u_z \nu_x) \sin(az) - (u_y \nu_z + u_z \nu_y) \cos(az) \end{aligned}$$

where az is the azimuth of observation. Equivalently,

$$\begin{aligned} A_1 &= \frac{1}{2}(M_{xx} - M_{yy}) \cos(2az) + M_{xy} \sin(2az) \\ A_2 &= M_{xz} \cos(az) + M_{yz} \sin(az) \\ A_3 &= -\frac{1}{2}(M_{xx} + M_{yy}) \end{aligned} \quad (\text{A5.3})$$

$$\begin{aligned} A_4 &= \frac{1}{2}(M_{xx} - M_{yy}) \sin(2az) - M_{xy} \cos(2az) \\ A_5 &= -M_{yz} \cos(az) + M_{xz} \sin(az) \end{aligned}$$

These equations are identical to (A5.2) which can be proven by using (18) together with (15) and (16). Note that the coefficients given in (A5.3) agree with the moment tensor elements as defined by Aki and Richards (1980; (A5.3) differs in sign with the coefficients of Langston (1981) due to conventions on displacements and Green's functions).

Note that either definition of the coefficients of the Green's functions can be used for the calculation of the displacement at the free surface, depending on whether the focal mechanism or the moment tensor is given. Here, equations (A5.3) and (A5.1) are used in order to develop an inversion scheme for the moment tensor elements. We

regroup and assume the presence of an isotropic component (ZEP \neq 0, REP \neq 0):

$$\begin{aligned} d_z(r, z=0, \omega) &= M_{xx} \left[\frac{ZSS}{2} \cos(2az) - \frac{ZDD}{2} + \frac{ZEP}{3} \right] \\ &+ M_{yy} \left[\frac{-ZSS}{2} \cos(2az) - \frac{ZDD}{2} + \frac{ZEP}{3} \right] \\ &+ M_{zz} \left[\frac{ZEP}{3} \right] \\ &+ M_{xy} [ZSS \sin(2az)] \\ &+ M_{xz} [ZDS \cos(az)] \\ &+ M_{yz} [ZDS \sin(az)] \end{aligned} \quad (\text{A5.4})$$

$$\begin{aligned} d_r(r, z=0, \omega) &= M_{xx} \left[\frac{RSS}{2} \cos(2az) - \frac{RDD}{2} + \frac{REP}{3} \right] \\ &+ M_{yy} \left[\frac{-RSS}{2} \cos(2az) - \frac{RDD}{2} + \frac{REP}{3} \right] \\ &+ M_{zz} \left[\frac{REP}{3} \right] \\ &+ M_{xy} [RSS \sin(2az)] \\ &+ M_{xz} [RDS \cos(az)] \\ &+ M_{yz} [RDS \sin(az)] \end{aligned} \quad (\text{A5.5})$$

$$\begin{aligned} d_\phi(r, z=0, \omega) &= M_{xx} \left[\frac{TSS}{2} \sin(2az) \right] \\ &+ M_{yy} \left[\frac{-TSS}{2} \sin(2az) \right] \\ &+ M_{xy} [-TSS \cos(2az)] \\ &+ M_{xz} [TDS \sin(az)] \\ &+ M_{yz} [-TDS \cos(az)] \end{aligned} \quad (\text{A5.6})$$

Equations (A5.4), (A5.5), and (A5.6) each set up a moment tensor inversion scheme. Equations (A5.4) and (A5.5) are formulated for the general case where the inversion expects a moment tensor that is a composition of an isotropic part and a deviatoric part. An inversion based on transverse data, (A5.6), cannot resolve M_{zz} . In such a case, we assume that the moment tensor is purely deviatoric and constrain $M_{zz} = -(M_{xx} + M_{yy})$. The same constraint can be applied to (A5.4) and (A5.5) in the case of

A Student's Guide to and Review of Moment Tensors

an inversion that looks for a pure deviatoric moment tensor (set formally $ZEP = REP = 0$ in (A5.4) and (A5.5), Dziewonski *et al.*, 1981).

From the last three equations we see that the observed displacement at the free surface is a linear combination of the station specific Green's functions, within the square brackets, with the moment tensor elements as scalar multipliers. We also note that if the source time function is known and a point source approximation is acceptable, the moment tensor elements are independent of frequency (linear inversion) and similar equations arise relating observed time histories to temporal Green's functions within the square brackets.

Next, we performed a simple moment tensor inversion using the vertical component of synthetic teleseismic P-wave first motion peak amplitudes as suggested by Stump and Johnson (1977). We assumed a pure deviatoric source ($ZEP = 0$ in (A5.4)).

Let az_1, \dots, az_n be azimuths of n different stations. Then the expressions in the square brackets of (A5.4) define components of a matrix as $a_{i1}(az_i), \dots, a_{i5}(az_i)$ for the i -th azimuth. A system of linear equation arises:

$$\begin{bmatrix} d_z(az_1) \\ \vdots \\ d_z(az_n) \end{bmatrix} = \begin{bmatrix} a_{11}(az_1) & \dots & a_{15}(az_1) \\ \vdots & \ddots & \vdots \\ a_{n1}(az_n) & \dots & a_{n5}(az_n) \end{bmatrix} \begin{bmatrix} M_{xx} \\ M_{yy} \\ M_{xy} \\ M_{zz} \\ M_{yz} \end{bmatrix} \quad (\text{A5.7})$$

For observations at more than 5 distinct azimuths, the system (A5.7) is overdetermined. The solution can be reached by the classical least squares approach. The five moment tensor elements can be determined by using the numerical stable singular value decomposition. We imposed the deviatoric constraint $M_{zz} = -(M_{xx} + M_{yy})$. Hence the inversion gives a purely deviatoric source. However, we were *not* constraining one eigenvalue as zero (double couple), letting the inversion tell us about double couple and CLVD components. The eigenvalues and eigenvectors can be calculated using the Householder transformation with further QL decomposition. The implementation of these numerical concepts was done using code by Press *et al.* (1987).

In the following, some results of inverting synthetic data are presented. First, Green's functions were calculated using a Haskell formalism for a simple half-space model ($V_p = 8$ km/sec, $V_s = 4.6$ km/sec and $\rho = 3.3$ g/cm³, $h = 30$ km). Figure A.3 shows the three basic Green's functions ZSS, ZDD, and ZDS. The assumed focal mechanism (Figure A.4: strike = 180°, dip = 40°, slip = 110°) is the same as used by Herrmann (1975, Figure 2). Teleseismic P-wave first motions were synthesized at 12 equidistant azimuths (epicentral distance = 50°). Note that an instrument response was not included in the synthetics. Due to the simple model and the fact that all stations are equidistant from the source, a correction for anelastic attenuation ($t^* = 0.7$) or geometrical spreading is not required. A correction for an extended source is not necessary since the moment used is 10²⁰ dyne-cm and the duration of the source time function is 0.2 sec. We used (A5.4) for time domain measurements.

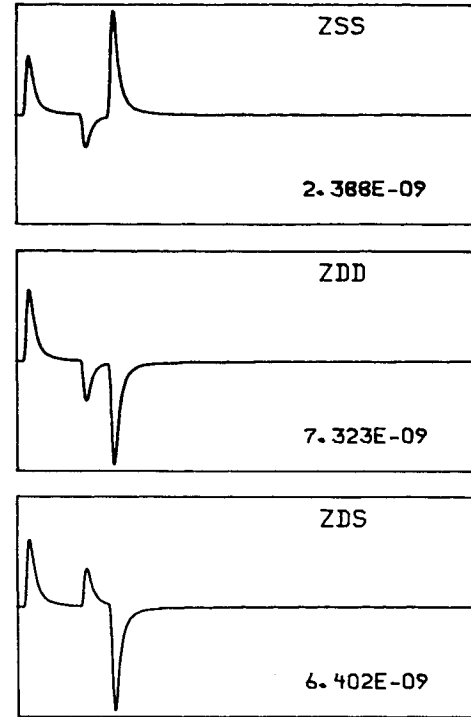


Fig. A.3. Synthetic Green's functions ZSS, ZDD, and ZDS (Herrmann and Wang, 1985) for a half-space model ($V_p = 8$ km/sec, $V_s = 4.6$ km/sec, $\rho = 3.3$ g/cm³, $h = 30$ km, $t^* = 0.7$) calculated by using the Haskell formalism. The time window ranges from 4.0 to 55.1 sec ($dt = 0.05$ sec). Maximum amplitudes are in cm (Appendix V).

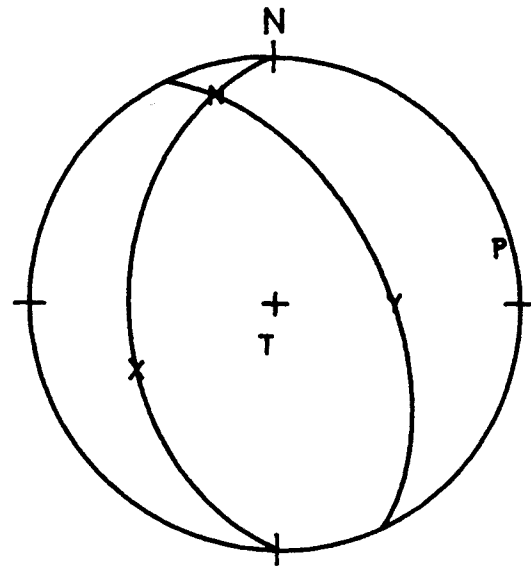


Fig. A.4. Assumed focal mechanism for the synthetic seismograms: strike = 180°, dip = 40°, slip = 110° (Appendix V).

TABLE A.7: RESULTS OF THE MOMENT TENSOR INVERSION (MAJOR COUPLE)

	Case 0	Case I	Case II	Case III	Case IV	Case V
M_{xx}	0	-0.037	-0.050	-0.109	-0.202	0.301
M_{yy}	-0.925	-0.902	-0.951	-0.966	-1.023	-1.091
M_{zz}	0.925	0.939	1.002	1.075	1.225	0.791
M_{xy}	-0.220	-0.199	-0.200	-0.194	-0.176	0.257
M_{xz}	-0.262	-0.262	-0.260	-0.264	-0.257	-0.172
M_{yz}	-0.163	-0.168	-0.162	-0.168	-0.156	-0.324
EV(NULL)	0.00	-0.04	-0.05	-0.11	-0.20	0.26
EV(T)	1.00	1.01	1.07	1.14	1.28	0.92
EV(P)	-1.00	-0.97	-1.02	-1.03	-1.08	-1.18
% of DC	100	92	90	81	69	56
% of CLVD	0	8	10	19	31	44
M_0	1.00	0.99	1.04	1.09	1.19	1.07
STRIKE	180.0	179.5	179.2	177.8	176.4	211.8
DIP	40.0	39.7	40.1	39.9	40.5	40.8
SLIP	110.0	109.0	107.8	106.1	103.2	123.1
STRIKE	334.6	335.4	336.5	337.2	339.3	351.1
DIP	52.8	52.9	52.2	51.9	50.8	56.8
SLIP	74.0	74.9	75.6	77.0	79.0	64.8
T (TRD)	192.7	194.9	194.7	196.8	198.2	209.7
T (PLG)	75.6	76.2	77.1	78.1	80.0	67.3
P (TRD)	75.9	76.1	76.7	76.4	77.1	98.8
P (PLG)	6.6	6.7	6.2	6.1	5.2	8.5

For Case 0, moment tensor elements are calculated from (18) assuming a double couple source (strike = 180° , dip = 40° , slip = 110°). The eigenvalues of the moment tensor corresponding to the null-, T-, and P-axes are shown as EV(NULL), EV(T), and EV(P), respectively. Equation (38) is used to determine the percentage of double couple or CLVD from the eigenvalues of the moment tensor. The seismic moment is calculated using (20). The orientation of the fault plane and auxiliary plane is given together with the trend and plunge of the T- and P-axes (Herrmann, 1975). Cases I - IV are for additive pseudo-random noise (0 %, 14 %, 28 %, and 56 %, respectively) in the synthetic seismograms at 12 different azimuths. Case V assumes that one of the 12 seismograms has a reversed polarity (0 % pseudo random noise).

Table A.7 displays the inversion results for the major couple. The moment tensor elements, the percentage of double couple and CLVD, the seismic moment, and the focal mechanism parameters are shown. For Case 0, the moment tensor elements were calculated from the given fault plane solution and (18). Next, three experiments were performed: 1.) synthetic seismograms were calculated using the Haskell method (Case I). Figure A.5a shows the vertical component of a synthetic seismogram at an azimuth of 0 degrees. 2.) Different amounts of pseudo-random noise were added to the synthetic seismograms calculated in Case I with amplitudes of $\pm 0.25 \times 10^{-9}$ cm (Case II, Figure A.5b), $\pm 0.5 \times 10^{-9}$ cm (Case III, Figure A.5c), and $\pm 1.0 \times 10^{-9}$ cm (Case IV, Figure A.5d). Averaged over the 12 azimuths, these noise levels correspond to 14 %, 28 %, and 56 % pseudo-random additive noise, respectively. 3.) The final experiment (Case V) relates to possible polarity errors of seismo-

graphs. Hence it was assumed that one of the 12 seismograms of Case I had a wrong polarity.

The theoretical focal parameters (Case 0) agree within the measurement errors with the observed ones (Case I). This justifies the technique. The effect of noise is to severely distort the moment tensor elements. The isotropic moment tensor components seem to be more sensitive to noise than the deviatoric ones. Notice that the moment tensor gains a contribution of a CLVD due to the noise. The percentage of CLVD versus double couple increases with increasing noise. The effect of random noise on the fault plane solution that is derived from the moment tensor elements is minor; i.e. the fault plane solution for the major double couple is very close to the original focal mechanism. However, with increasing noise, the fault plane solution deteriorates. 8 % polarization errors in otherwise perfect data lead to worse results than 56 % additive random noise (Case IV). A doubling of the

REFERENCES

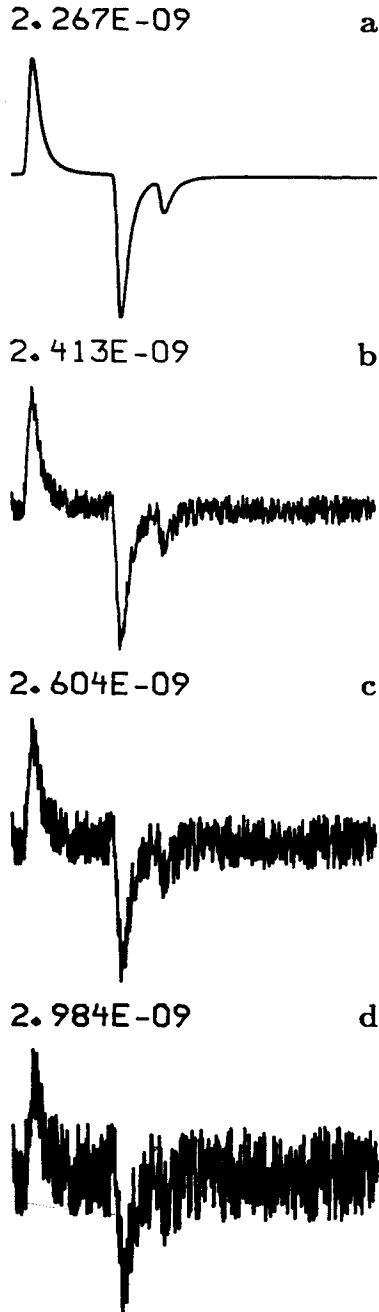


Fig. A.5. Vertical components of synthetic teleseismic seismograms at 50 degrees and azimuth of 0° . The time window ranges from 4.0 to 29.6 sec ($dt = 0.05$ sec). Maximum amplitudes are in cm. (a) No pseudo-random noise added; (b) - (d) pseudo-random noise is added with amplitudes of $\pm 0.25 \times 10^{-9}$ cm, $\pm 0.50 \times 10^{-9}$ cm, $\pm 1.0 \times 10^{-9}$ cm, respectively (Appendix V).

polarization errors gives meaningless results. Due to the setup of the experiment, a minor couple would be a pure artifact of the noise.

Agnew, D., J. Berger, R. Buland, W. Farrell, and F. Gilbert (1976). International deployment of accelerometers: a network for very long-period seismology, *EOS, Trans. Am. Geophys. Union* **57**, 180-188.

Aki, K. and P. G. Richards (1980). *Quantitative Seismology: Theory and Methods*, W. H. Freeman and Co., New York, San Francisco, 932 pp.

Arfken, G. (1985). *Mathematical Methods for Physicists*, 3rd ed., Academic Press Inc., Orlando, Florida, 985 pp.

Backus, G. E. (1977a). Interpreting the seismic glut moments of total degree two or less, *Geophys. J. R. Astr. Soc.* **51**, 1-25.

Backus, G. E. (1977b). Seismic sources with observable glut moments of spatial degree two, *Geophys. J. R. Astr. Soc.* **51**, 27-45.

Backus, G. and M. Mulcahy (1976). Moment tensors and other phenomenological descriptions of seismic sources - I. continuous displacements, *Geophys. J. R. Astr. Soc.* **46**, 341-361.

Ben-Menahem, A. and S. J. Singh (1968). Eigenvector expansions of Green's dyads with applications to geophysical theory, *Geophys. J. R. Astr. Soc.* **16**, 417-452.

Ben-Menahem, A. and S. J. Singh (1981). *Seismic Waves and Sources*, Springer Verlag, New York, 1108 pp.

Bullen, K. E. and B. A. Bolt (1985). *An Introduction to the Theory of Seismology*, 4th ed., Cambridge University Press, Cambridge, 499 pp.

Burdick, L. J. and G. R. Mellman (1976). Inversion of the body waves from the Borrego Mountain earthquake to the source mechanism, *Bull. Seism. Soc. Am.* **66**, 1485-1499.

Burridge, R., E. R. Lapwood, and L. Knopoff (1964). First motions from seismic sources near a free surface, *Bull. Seism. Soc. Am.* **54**, 1889-1913.

Christensen, D. H. and L. J. Ruff (1985). Analysis of the trade-off between hypocentral depth and source time function, *Bull. Seism. Soc. Am.* **75**, 1637-1656.

Claerbout, J. F. and F. Muir (1973). Robust modeling with erratic data, *Geophysics* **38**, 826-844.

Dziewonski, A. M. and F. Gilbert (1974). Temporal variation of the seismic moment tensor and the evidence of precursive compression for two deep earthquakes, *Nature* **247**, 185-188.

- Dziewonski, A. M. and J. H. Woodhouse (1983a). Studies of the seismic source using normal-mode theory, in *Earthquakes: Observation, Theory and Interpretation*, H. Kanamori and E. Boschi, Editors, North-Holland, Amsterdam, New York, Oxford, 608 pp.
- Dziewonski, A. M. and J. H. Woodhouse (1983b). An experiment in systematic study of global seismicity: centroid-moment tensor solutions for 201 moderate and large earthquakes of 1981, *J. Geophys. Res.* **88**, 3247-3271.
- Dziewonski, A. M., T.-A. Chou, and J. H. Woodhouse (1981). Determination of earthquake source parameters from waveform data for studies of global and regional seismicity, *J. Geophys. Res.* **86**, 2825-2852.
- Dziewonski, A. M., A. Friedman, D. Giardini, and J. H. Woodhouse (1983a). Global seismicity of 1982: centroid-moment tensor solutions for 308 earthquakes, *Phys. Earth Planet. Interiors* **33**, 76-90.
- Dziewonski, A. M., A. Friedman, and J. H. Woodhouse (1983b). Centroid-moment tensor solutions for January-March 1983, *Phys. Earth Planet. Interiors* **33**, 71-75.
- Dziewonski, A. M., J. E. Franzen, and J. H. Woodhouse (1983c). Centroid-moment tensor solutions for April-June 1983, *Phys. Earth Planet. Interiors* **33**, 243-249.
- Dziewonski, A. M., J. E. Franzen, and J. H. Woodhouse (1984a). Centroid-moment tensor solutions for July-September 1983, *Phys. Earth Planet. Interiors* **34**, 1-8.
- Dziewonski, A. M., J. E. Franzen, and J. H. Woodhouse (1984b). Centroid-moment tensor solutions for October-December 1983, *Phys. Earth Planet. Interiors* **34**, 129-136.
- Dziewonski, A. M., J. E. Franzen, and J. H. Woodhouse (1984c). Centroid-moment tensor solutions for January-March 1984, *Phys. Earth Planet. Interiors* **34**, 209-219.
- Dziewonski, A. M., J. E. Franzen, and J. H. Woodhouse (1985a). Centroid-moment tensor solutions for April-June 1984, *Phys. Earth Planet. Interiors* **37**, 87-96.
- Dziewonski, A. M., J. E. Franzen, and J. H. Woodhouse (1985b). Centroid-moment tensor solutions for July-September 1984, *Phys. Earth Planet. Interiors* **38**, 203-213.
- Dziewonski, A. M., J. E. Franzen, and J. H. Woodhouse (1985c). Centroid-moment tensor solutions for October-December 1984, *Phys. Earth Planet. Interiors* **39**, 147-156.
- Dziewonski, A. M., J. E. Franzen, and J. H. Woodhouse (1985d). Centroid-moment tensor solutions for January-March 1985, *Phys. Earth Planet. Interiors* **40**, 249-258.
- Dziewonski, A. M., J. E. Franzen, and J. H. Woodhouse (1986a). Centroid-moment tensor solutions for April-June 1985, *Phys. Earth Planet. Interiors* **41**, 215-224.
- Dziewonski, A. M., J. E. Franzen, and J. H. Woodhouse (1986b). Centroid-moment tensor solutions for July-September 1985, *Phys. Earth Planet. Interiors* **42**, 205-214.
- Dziewonski, A. M., J. E. Franzen, and J. H. Woodhouse (1986c). Centroid-moment tensor solutions for October-December 1985, *Phys. Earth Planet. Interiors* **43**, 185-195.
- Dziewonski, A. M., G. Ekström, J. E. Franzen, and J. H. Woodhouse (1987a). Centroid-moment tensor solutions for January-March 1986, *Phys. Earth Planet. Interiors* **45**, 1-10.
- Dziewonski, A. M., G. Ekström, J. E. Franzen, and J. H. Woodhouse (1987b). Global seismicity of 1977: centroid-moment tensor solutions for 471 earthquakes, *Phys. Earth Planet. Interiors* **45**, 11-36.
- Dziewonski, A. M., G. Ekström, J. E. Franzen, and J. H. Woodhouse (1987c). Centroid-moment tensor solutions for July-September 1986, *Phys. Earth Planet. Interiors* **46**, 305-315.
- Dziewonski, A. M., G. Ekström, J. E. Franzen, and J. H. Woodhouse (1987d). Global seismicity of 1978: centroid-moment tensor solutions for 512 earthquakes *Phys. Earth Planet. Interiors* **46**, 316-342.
- Dziewonski, A. M., G. Ekström, J. H. Woodhouse and G. Zwart (1987e). Centroid-moment tensor solutions for October-December 1986, *Phys. Earth Planet. Interiors* **48**, 5-17.
- Dziewonski, A. M., G. Ekström, J. E. Franzen, and J. H. Woodhouse (1987f). Global seismicity of 1979: centroid-moment tensor solutions for 524 earthquakes *Phys. Earth Planet. Interiors* **48**, 18-46.
- Ekström, G. and A. M. Dziewonski (1985). Centroid-moment tensor solutions for 35 earthquakes in Western North America (1977-1983), *Bull. Seism. Soc. Am.* **75**, 23-39.
- Ekström, G., A. M. Dziewonski, and J. H. Woodhouse (1987). Centroid-moment tensor solutions for the 51 IASPEI selected earthquakes, 1980-1984, *Phys. Earth Planet. Interiors* **47**, 62-66.
- Engdahl, E. R. and H. Kanamori (1980). Determination of earthquake parameters, *EOS, Trans. Am. Geophys. Union* **61**, 60-65.

A Student's Guide to and Review of Moment Tensors

- Evison, F. F. (1963). Earthquakes and faults, *Bull. Seism. Soc. Am.* **53**, 873-891.
- Faddeeva (1959). *Computational Methods of Linear Algebra*, Dover, New York, 252 pp.
- Fitch, T. J. (1981). Correction and addition to 'Estimation of the seismic moment tensor from teleseismic body wave data with applications to intraplate and mantle earthquakes' by T. J. Fitch, D. W. McCowan, and M. W. Shields, *J. Geophys. Res.* **86**, 9375-9376.
- Fitch, T. J., D. W. McCowan, and M. W. Shields (1980). Estimation of the seismic moment tensor from teleseismic body wave data with applications to intraplate and mantle earthquakes, *J. Geophys. Res.* **85**, 3817-3828.
- Fitch, T. J., R. G. North, and M. W. Shields (1981). Focal depths and moment tensor representations of shallow earthquakes associated with the great Sumba earthquake, *J. Geophys. Res.* **86**, 9357-9374.
- Geller, R. J. (1976). Body force equivalents for stress-drop seismic sources, *Bull. Seism. Soc. Am.* **66**, 1801-1804.
- Giardini, D. (1984). Systematic analysis of deep seismicity: 200 centroid-moment tensor solutions for earthquakes between 1977 and 1980, *Geophys. J. R. Astr. Soc.* **77**, 883-914.
- Gilbert, F. (1970). Excitation of the normal modes of the earth by earthquake sources, *Geophys. J. R. Astr. Soc.* **22**, 223-226.
- Gilbert, F. (1973). Derivation of source parameters from low-frequency spectra, *Phil. Trans. R. Soc. A* **274**, 369-371.
- Gilbert, F. and R. Buland (1976). An enhanced deconvolution procedure for retrieving the seismic moment tensor from a sparse network, *Geophys. J. R. Astr. Soc.* **47**, 251-255.
- Gilbert, F. and A. M. Dziewonski (1975). An application of normal mode theory to the retrieval of structural parameters and source mechanisms from seismic spectra, *Phil. Trans. R. Soc. A* **278**, 187-269.
- Gomberg, J. S. and T. G. Masters (1988). Waveform modeling using locked-mode synthetic and differential seismograms: application to determination of the structure of Mexico, *Geophys. J.* **94**, 193-218.
- Hagiwara, T. (1958). A note on the theory of the electromagnetic seismograph, *Bull. Earthquake Res. Inst. Tokyo Univ.* **36**, 139-164.
- Harkrider, D. G. (1964). Surface waves in multilayered elastic media, 1. Rayleigh and Love waves from buried sources in a multilayered elastic half-space, *Bull. Seism. Soc. Am.* **54**, 627-679.
- Harkrider, D. G. (1970). Surface waves in multilayered elastic media, 2. Higher mode spectra and spectral ratios from point sources in plane layered earth models, *Bull. Seism. Soc. Am.* **60**, 1937-1987.
- Harkrider, D. G. (1976). Potentials and displacements for two theoretical seismic sources, *Geophys. J. R. Astr. Soc.* **47**, 97-133.
- Herrmann, R. B. (1975). A student's guide to the use of P and S wave data for focal mechanism determination, *Earthquake Notes* **46**, 29-39.
- Herrmann, R. B. and C. Y. Wang (1985). A comparison of synthetic seismograms, *Bull. Seism. Soc. Am.* **75**, 41-56.
- Hirasawa, T. and W. Stauder, S.J. (1965). On the seismic body waves from a finite moving source, *Bull. Seism. Soc. Am.* **55**, 237-262.
- Honda, H. (1962). Earthquake mechanism and seismic waves, *Geophysical Notes, Geophys. Inst., Fac. of Science, Tokyo Univ.* **15**, 1-97.
- Kanamori, H. and J. W. Given (1981). Use of long-period surface waves for rapid determination of earthquake-source parameters, *Phys. Earth Planet. Interiors* **27**, 8-31.
- Kanamori, H. and J. W. Given (1982). Use of long-period surface waves for rapid determination of earthquake source parameters: 2. Preliminary determination of source mechanisms of large earthquakes ($M_s \geq 6.5$) in 1980, *Phys. Earth Planet. Interiors* **30**, 260-268.
- Kennett, B. L. N. (1983). *Seismic Wave Propagation in Stratified Media*, Cambridge University Press, Cambridge, 342 pp.
- Kennett, B. L. N. (1988). Radiation from a moment-tensor source, in *Seismological Algorithms - Computational Methods and Computer Programs*, D. J. Doornbos, Editor, Academic Press, San Diego, California, 427-441.
- Kikuchi, M. and H. Kanamori (1982). Inversion of complex body waves, *Bull. Seism. Soc. Am.* **72**, 491-506.
- Knopoff, L. and M. J. Randall (1970). The compensated linear-vector dipole: a possible mechanism for deep earthquakes, *J. Geophys. Res.* **75**, 4957-4963.
- Landisman, M., A. Dziewonski, and Y. Sato (1969). Recent improvements in the analysis of surface wave observations, *Geophys. J. R. Astr. Soc.* **17**, 369-403.

- Langston, C. A. (1981). Source inversion of seismic waveforms: The Koyana, India, earthquakes of 13 September 1967, *Bull. Seism. Soc. Am.* **71**, 1-24.
- Langston, C. A. and D. V. Helmberger (1975). A procedure for modeling shallow dislocation sources, *Geophys. J. R. Astr. Soc.* **42**, 117-130.
- Lawson, C. H. and R. J. Hanson (1974). *Solving Least Squares Problems*, Prentice-Hall, Englewood Cliffs, New Jersey.
- Lay, T., J. W. Given, and H. Kanamori (1982). Long-period mechanism of the 8 November 1980 Eureka, California, earthquake, *Bull. Seism. Soc. Am.* **72**, 439-456.
- Lundgren, P. R., E. A. Okal, and S. Stein (1988). Body-wave deconvolution for variable source parameters; application to the 1978 December 6 Kuriles earthquake, *Geophys. J.* **94**, 171-180.
- Maruyama, T. (1964). Statical elastic dislocations in an infinite and semi-infinite medium, *Bull. Earthquake Res. Inst.* **42**, 289-368.
- McCowan, D. W. (1976). Moment tensor representation of surface wave sources, *Geophys. J. R. Astr. Soc.* **44**, 595-599.
- McCowan, D. W. and R. T. Lacoss (1978). Transfer functions for the seismic research observatory seismograph system, *Bull. Seism. Soc. Am.* **68**, 501-512.
- McKenzie, D. P. (1969). The relation between fault plane solutions for earthquakes and the directions of the principal stresses, *Bull. Seism. Soc. Am.* **59**, 591-601.
- Mendiguren, J. A. (1977). Inversion of surface wave data in source mechanism studies, *J. Geophys. Res.* **82**, 889-894.
- Nakanishi, I. and H. Kanamori (1982). Effects of lateral heterogeneity and source process time on the linear moment tensor inversion of long-period Rayleigh waves, *Bull. Seism. Soc. Am.* **72**, 2063-2080.
- Nakanishi, I. and H. Kanamori (1984). Source mechanisms of twenty-six large, shallow earthquakes ($M_S \geq 6.5$) during 1980 from P-wave first motion and long-period Rayleigh wave data, *Bull. Seism. Soc. Am.* **74**, 805-818.
- O'Connell, D. R. H. and L. R. Johnson (1988). Second order moment tensors of microearthquakes at The Geysers geothermal field, California, *Bull. Seism. Soc. Am.* **78**, 1674-1692.
- Okal, E. A. and R. J. Geller (1979). On the observability of isotropic seismic sources: the July 31, 1970 Colombian earthquake, *Phys. Earth Planet. Interiors* **18**, 176-196.
- Patton, H. (1980). Reference point equalization method for determining the source and path effects of surface waves, *J. Geophys. Res.* **85**, 821-848.
- Patton, H. and K. Aki (1979). Bias in the estimate of seismic moment tensor by the linear inversion method, *Geophys. J. R. Astr. Soc.* **59**, 479-495.
- Press, W. H., B. P. Flannery, S. A. Teukolsky, and W. T. Vetterling (1987). *Numerical Recipes: The Art of Scientific Computing*, Cambridge University Press, Cambridge, 818 pp.
- Randall, M. J. and L. Knopoff (1970). The mechanism at the focus of deep earthquakes, *J. Geophys. Res.* **75**, 4965-4976.
- Reid, H. F. (1910). Elastic rebound theory, *Univ. Calif. Publ., Bull. Dept. Geol. Sci.* **6**, 413-433.
- Romanowicz, B. (1981). Depth resolution of earthquakes in central Asia by moment tensor inversion of long-period Rayleigh waves: Effects of phase velocity variations across Eurasia and their calibration, *J. Geophys. Res.* **86**, 5963-5984.
- Saito, M. (1967). Excitation of free oscillations and surface waves by a point source in a vertically heterogeneous earth, *J. Geophys. Res.* **72**, 3689-3699.
- Satake, K. (1985). Effects of station coverage on moment tensor inversion, *Bull. Seism. Soc. Am.* **75**, 1657-1667.
- Scott, D. R. and H. Kanamori (1985). On the consistency of moment tensor source mechanisms with first-motion data, *Phys. Earth Planet. Interiors* **37**, 97-107.
- Silver, P. G. and T. H. Jordan (1982). Optimal estimation of scalar seismic moment, *Geophys. J. R. Astr. Soc.* **70**, 755-787.
- Sipkin, S. A. (1982). Estimation of earthquake source parameters by the inversion of waveform data: synthetic waveforms, *Phys. Earth Planet. Interiors* **30**, 242-255.
- Sipkin, S. A. (1986). Interpretation of non-double-couple earthquake mechanisms derived from moment tensor inversion, *J. Geophys. Res.* **91**, 531-547.
- Sipkin, S. A. (1987). Moment tensor solutions estimated using optimal filter theory for 51 selected earthquakes, 1980-1984, *Phys. Earth Planet. Interiors* **47**, 67-79.
- Snieder, R. and B. Romanowicz (1988). A new formalism for the effect of lateral heterogeneity on normal modes and surface waves - I: isotropic perturbations, perturbations of interfaces and gravitational perturbations, *Geophys. J.* **92**, 207-222.

A Student's Guide to and Review of Moment Tensors

- Strelitz, R. A. (1978). Moment tensor inversions and source models, *Geophys. J. R. Astr. Soc.* **52**, 359-364.
- Strelitz, R. A. (1980). The fate of the downgoing slab: A study of the moment tensors from body waves of complex deep-focus earthquakes, *Phys. Earth Planet. Interiors* **21**, 83-96.
- Stump, B. W. and L. R. Johnson (1977). The determination of source properties by the linear inversion of seismograms, *Bull. Seism. Soc. Am.* **67**, 1489-1502.
- Vasco, D. W. and L. R. Johnson (1988). Inversion of waveforms for extreme source models with an application to the isotropic moment tensor component, in *Regional Studies with Broadband Data*, T. V. McEvelly and L. R. Johnson, Editors, Report No. 1, Air Force Geophysics Laboratory AFGL-TR-88-0131.
- Wallace, T. C. (1985). A reexamination of the moment tensor solutions of the 1980 Mammoth Lakes earthquakes, *J. Geophys. Res.* **90**, 11,171-11,176.
- Wallace, T. C., D. V. Helmberger, and G. R. Mellman (1981). A technique for the inversion of regional data in source parameter studies, *J. Geophys. Res.* **86**, 1679-1685.
- Wang C. Y. and R. B. Herrmann (1980). A numerical study of P-, SV-, and SH-wave generation in a plane layered medium, *Bull. Seism. Soc. Am.* **70**, 1015-1036.
- Ward, S. N. (1980a). Body wave calculations using moment tensor sources in spherically symmetric, inhomogeneous media, *Geophys. J. R. Astr. Soc.* **60**, 53-66.
- Ward, S. N. (1980b). A technique for the recovery of the seismic moment tensor applied to the Oaxaca, Mexico earthquake of November 1978, *Bull. Seism. Soc. Am.* **70**, 717-734.

Received June 23, 1988
Revised October 4, 1988
Accepted November 1, 1988